AI for Digital breast Tomosynthesis

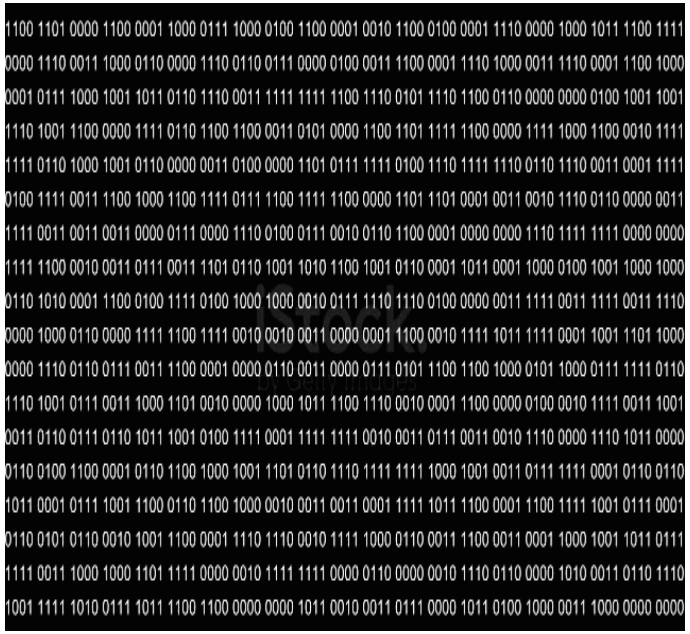

Prof. Giovanni Mettivier

Mammography

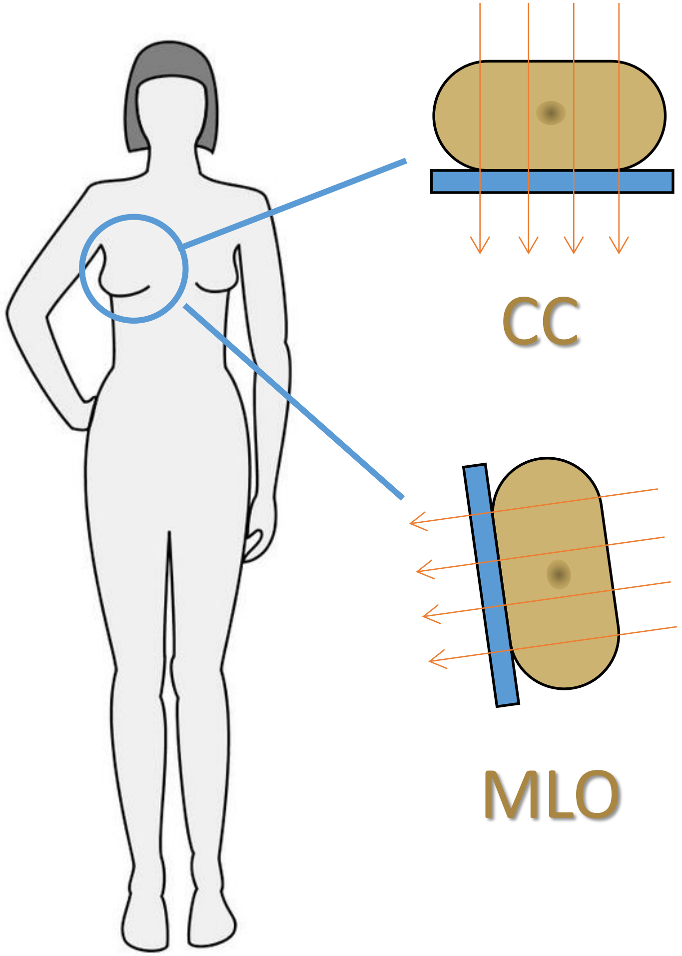

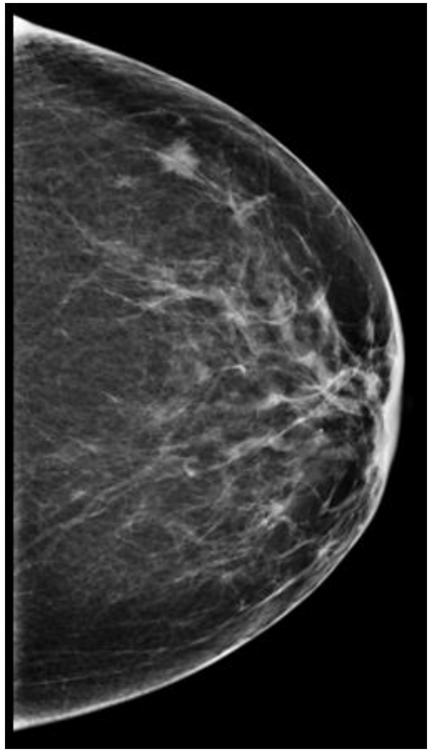

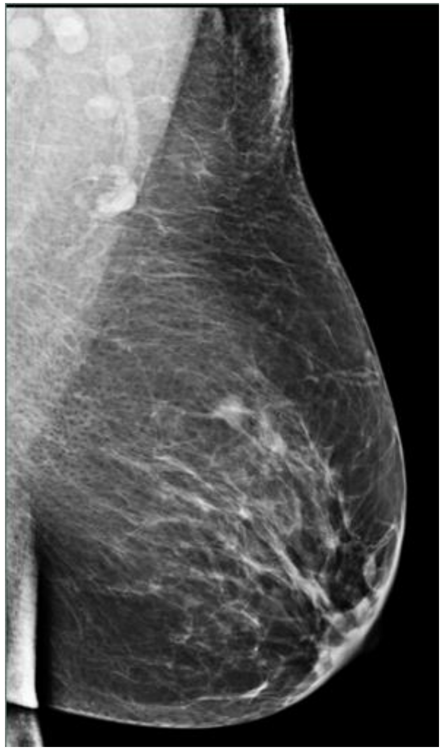

CC MLO

Mammography

"However, due to the two-dimensional nature of projection imaging, mammography is limited by overlapping tissue

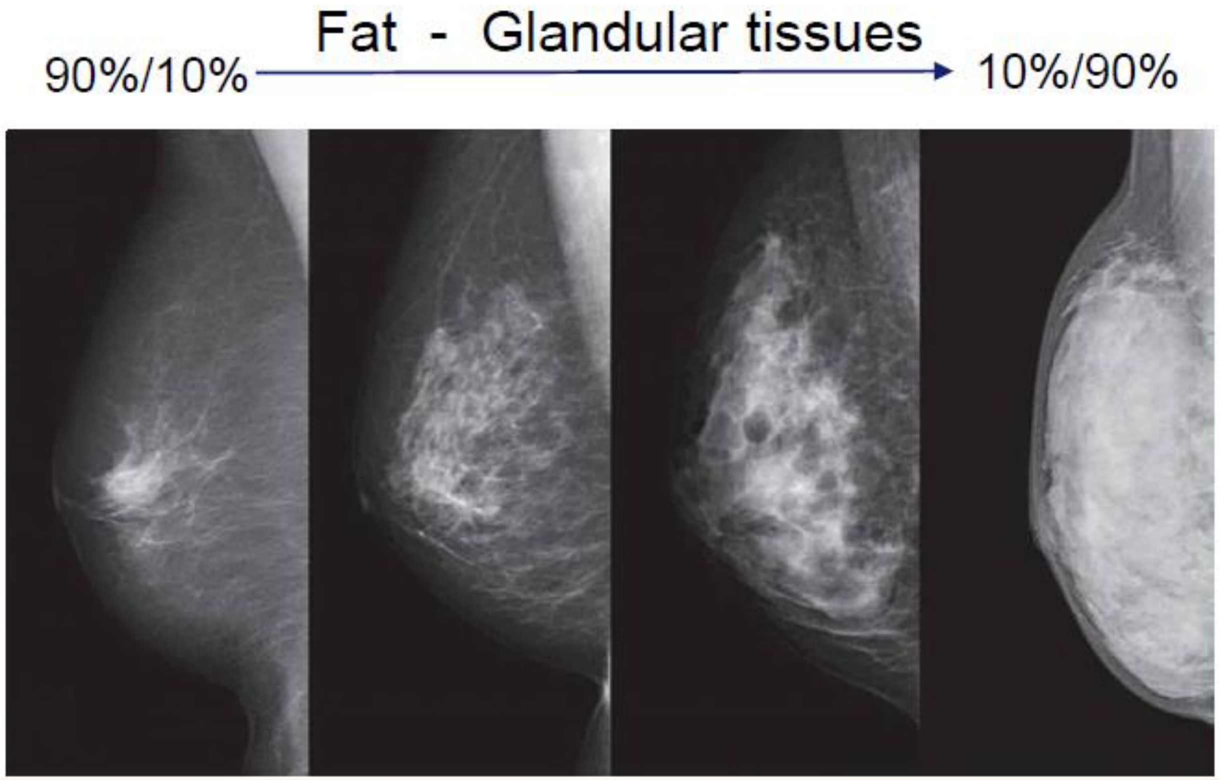

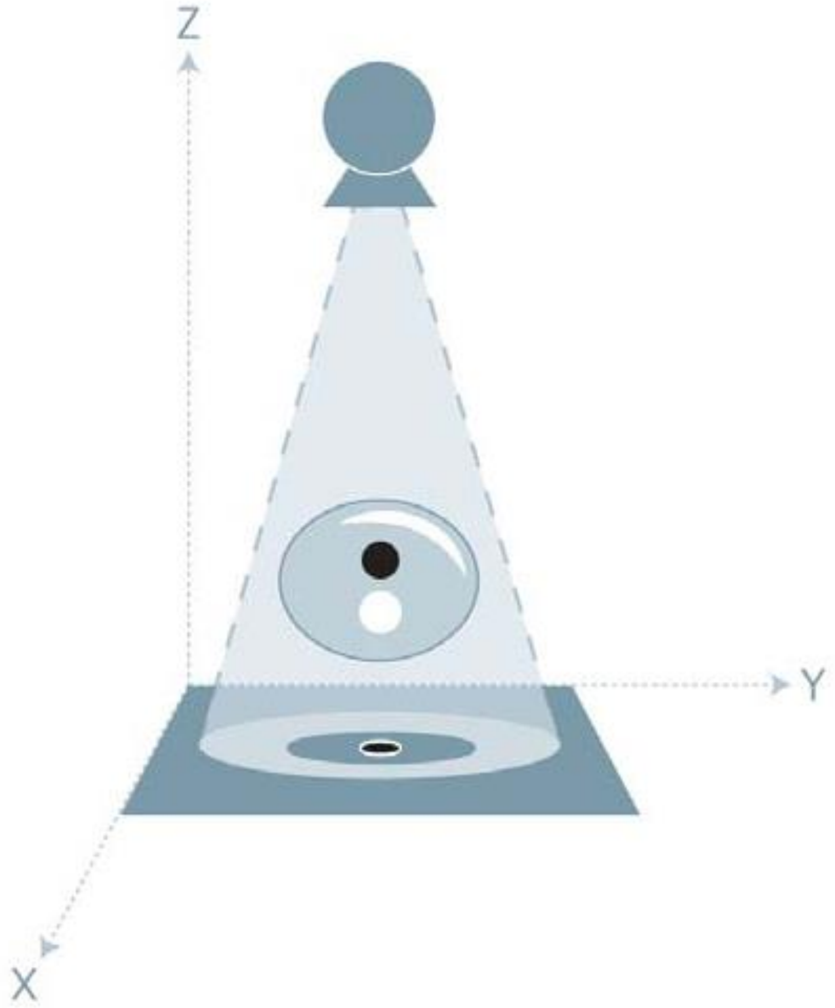

J. Baker & J. Lo, Duke University in Durham, NC, USA
A. Hebecker , T. Mertelmeier & J. Orman, Siemens Medical Solutions, Erlangen, Germany

Digital Breast Tomosynthesis

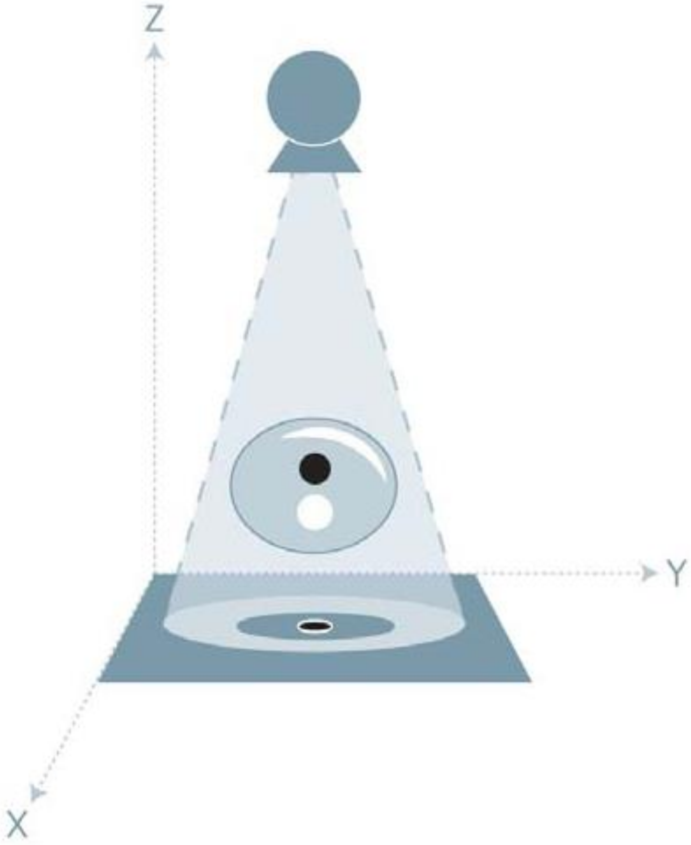

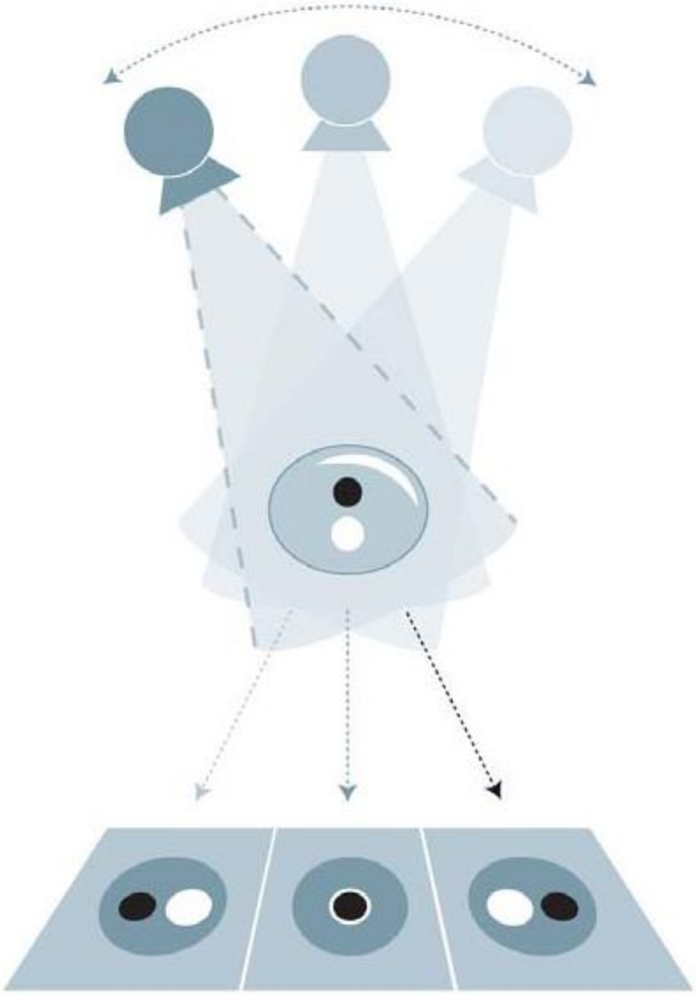

www.siemens.com/healthcare

Digital Breast Tomosynthesis

3D Breast Tomosynthesis –
White Paper – www.siemens.com/healthcare

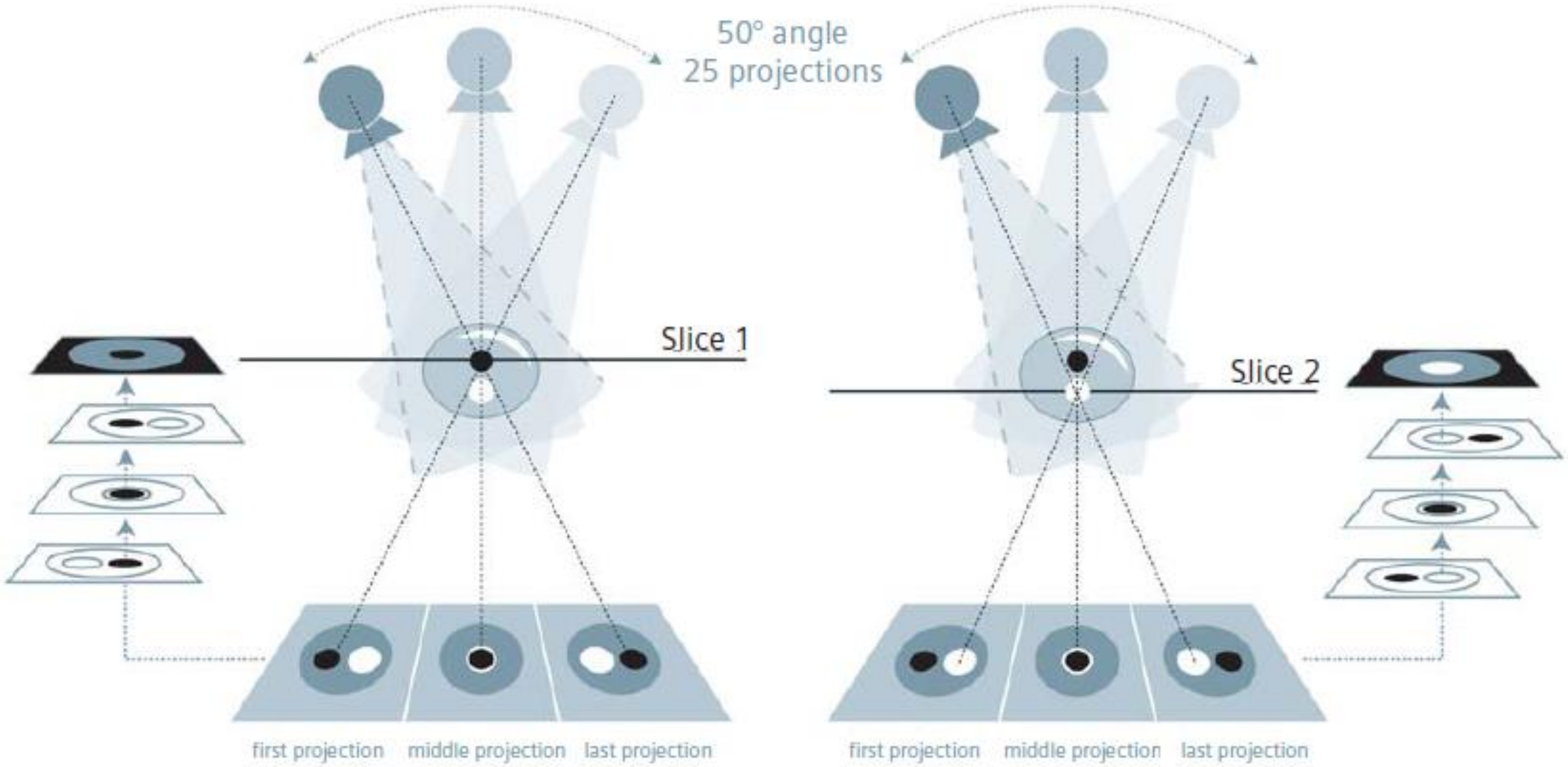

Digital Breast Tomosynthesis

Acquisition

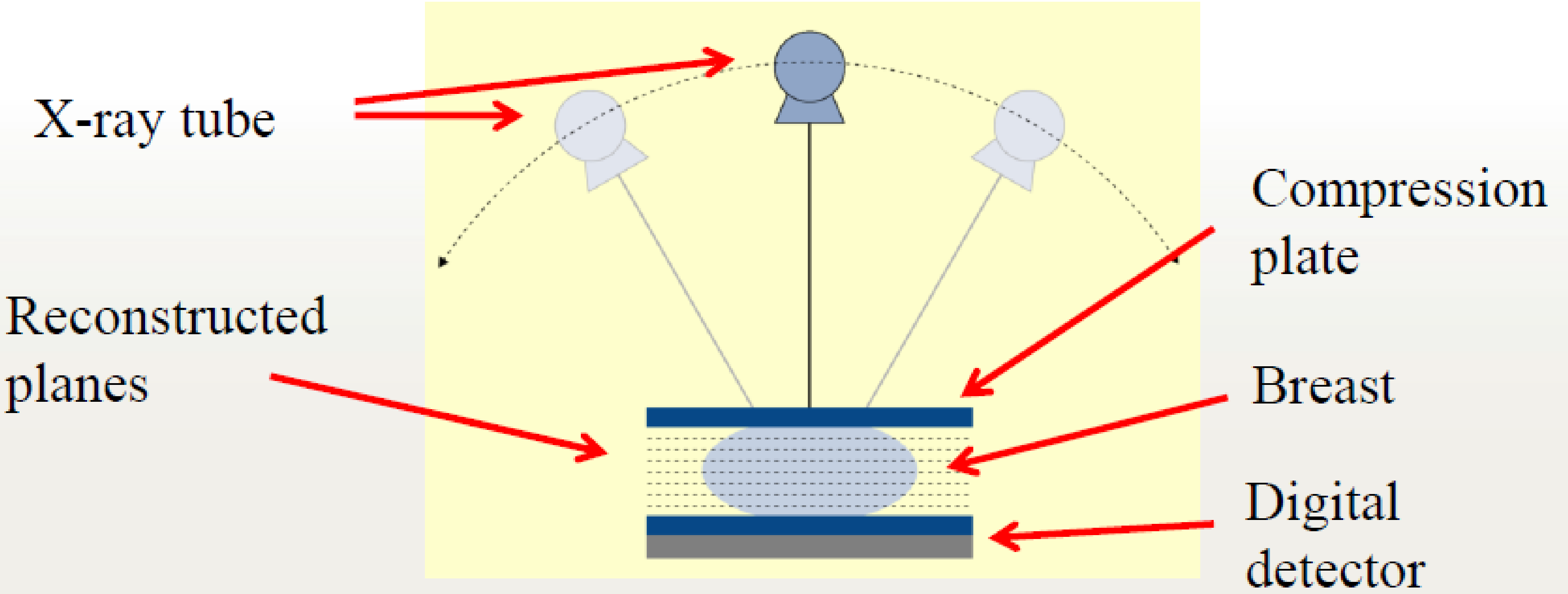

- X-ray tube moves in an arc across the breast
- Series of low dose images are acquired at different angles
- Total dose similar to single view breast exam

A. Smith, www.hologic.com

A malignancy easily missed with conventional 2D mammography was clearly seen with Hologic 3D Mammography

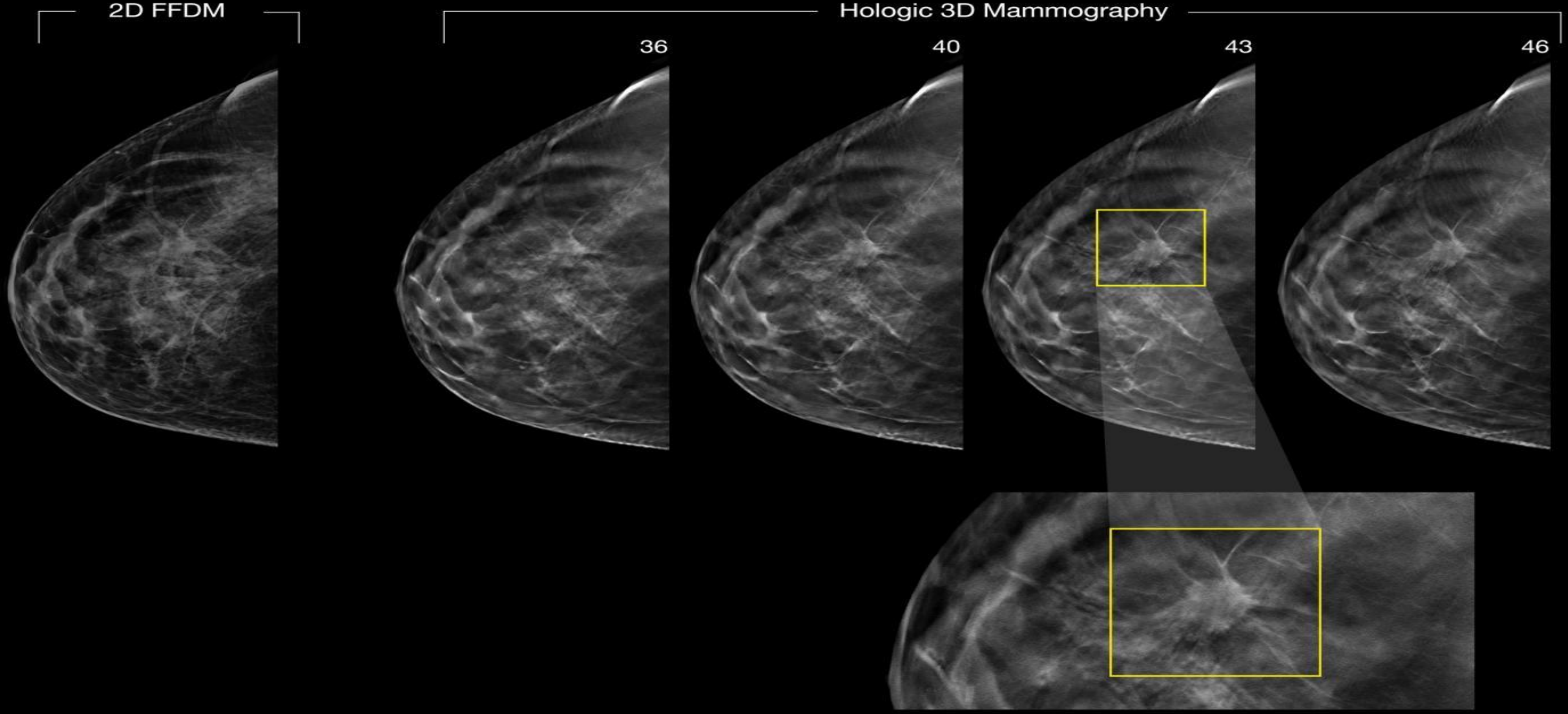

PROBLEMATICHE

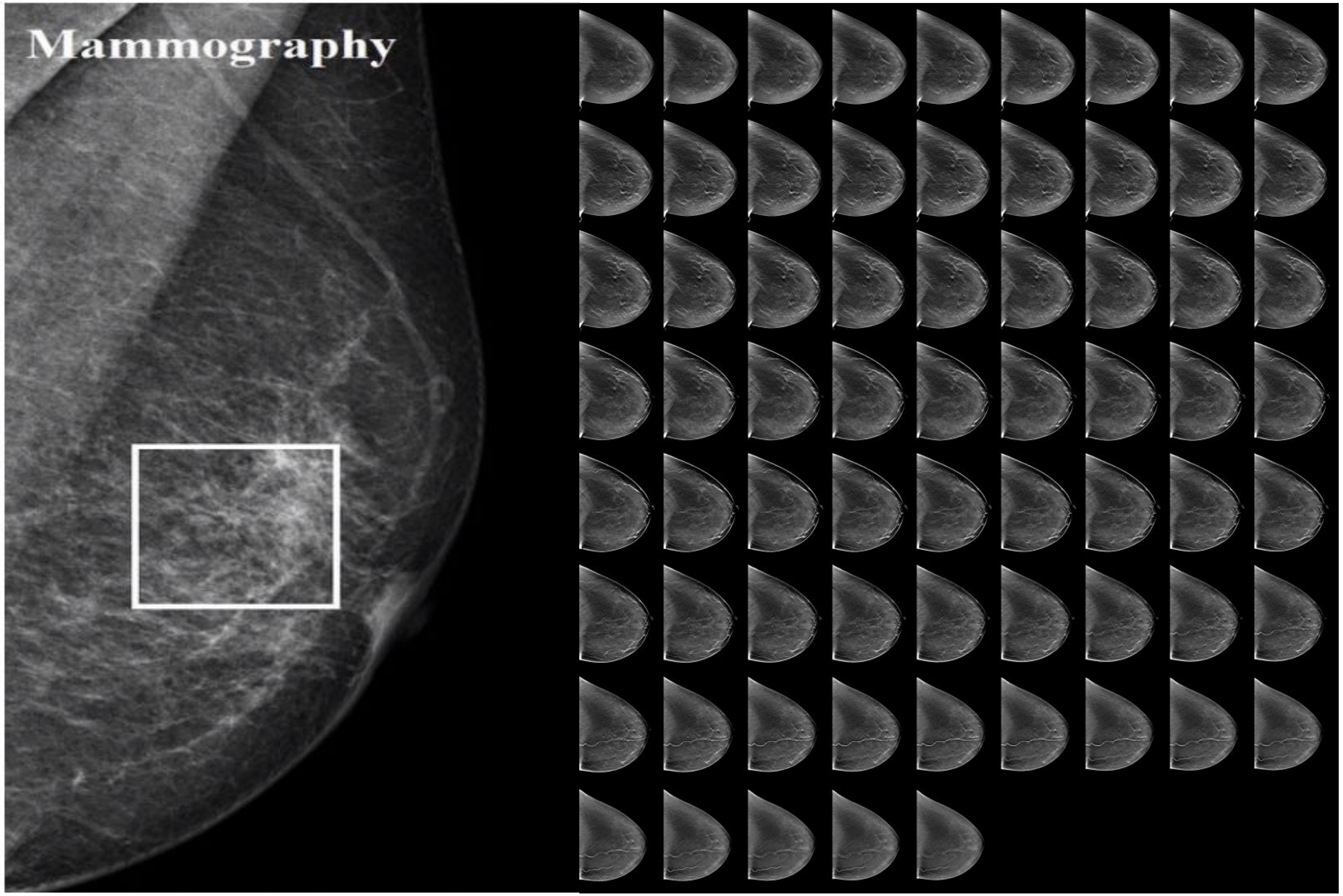

Maggior numero di immagini da analizzare

Maggior carico lavorativo per il medico radiologo

Maggiore probabilità di effettuare una diagnosi erronea o incompleta

Classificazione delle DBT

- Meno stress lavorativo a carico del personale medico
- Meno stress psicologico ai pazienti
- Riduzione dei costi per le aziende ospedaliere

McDonald RJ et al, "**The effects of changes in utilization and technological advancements of cross-sectional imaging on radiologist workload**." Acad Radiol. Sep;22(9):1191-8 (2015).

Aim of Project

DeepLook is a national Technological Transfer project founded by INFN and started in 2022.

The aim is to implement a deep learning architecture for Computed Aided Detection (CAD), based on neural networks developed with deep learning methods, for the automatic detection and classification of breast lesions in DBT images.

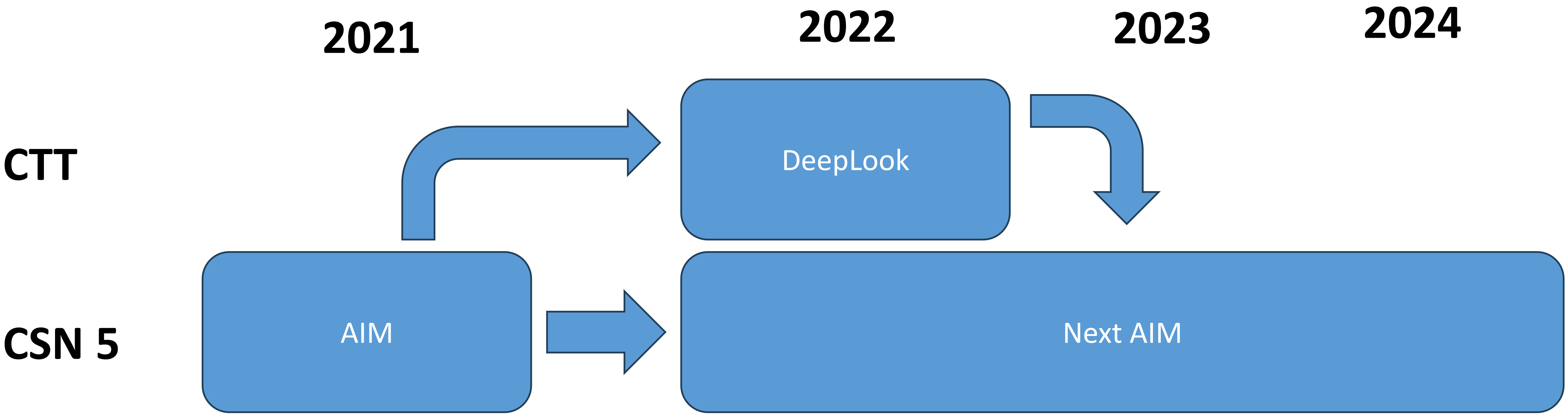

INFN Napoli
G. Mettivier, R. Ricciardi, D. Esposito, P. Russo, M. Staffa, S. Clemente

INFN Bologna
D. Remondini and Nico Curti

INFN Ferrata
G.釘aternò

ASL CUNEO 1
M. Porzio

AORN Cardarelli
S. Minelli, E. Antignani, A. Santoro

IFO Regina Elena
V. Landoni, P. Ordonez, F. Ferranti, L . Greco, M. Masi

DeepLook Dataset

Dataset (Hospital site)	Expected final no. of patients	Present no. of patients	Total no. DBT slices	TP	TN	Bio	DBT scanner	View	FFDM available
AORN Cardarelli	250	200	7466	3528	3938	Yes	Giotto Class 40000	CC, MLO	Yes
IRCSS R. E.	250	96	2915	1541	1374	Yes	Giotto Class 40000	MLO	No
ASL Cuneo 1	500	10	-	-	-	Yes	Multi	CC, MLO	
AOU Fed II	250	-	-	-	-	No	Hologic Selenia Dimensions	CC, MLO	Yes
Duke	349	349	21518	14057	7461				

All the images were annotated by dedicated breast radiologists

Duke Dataset

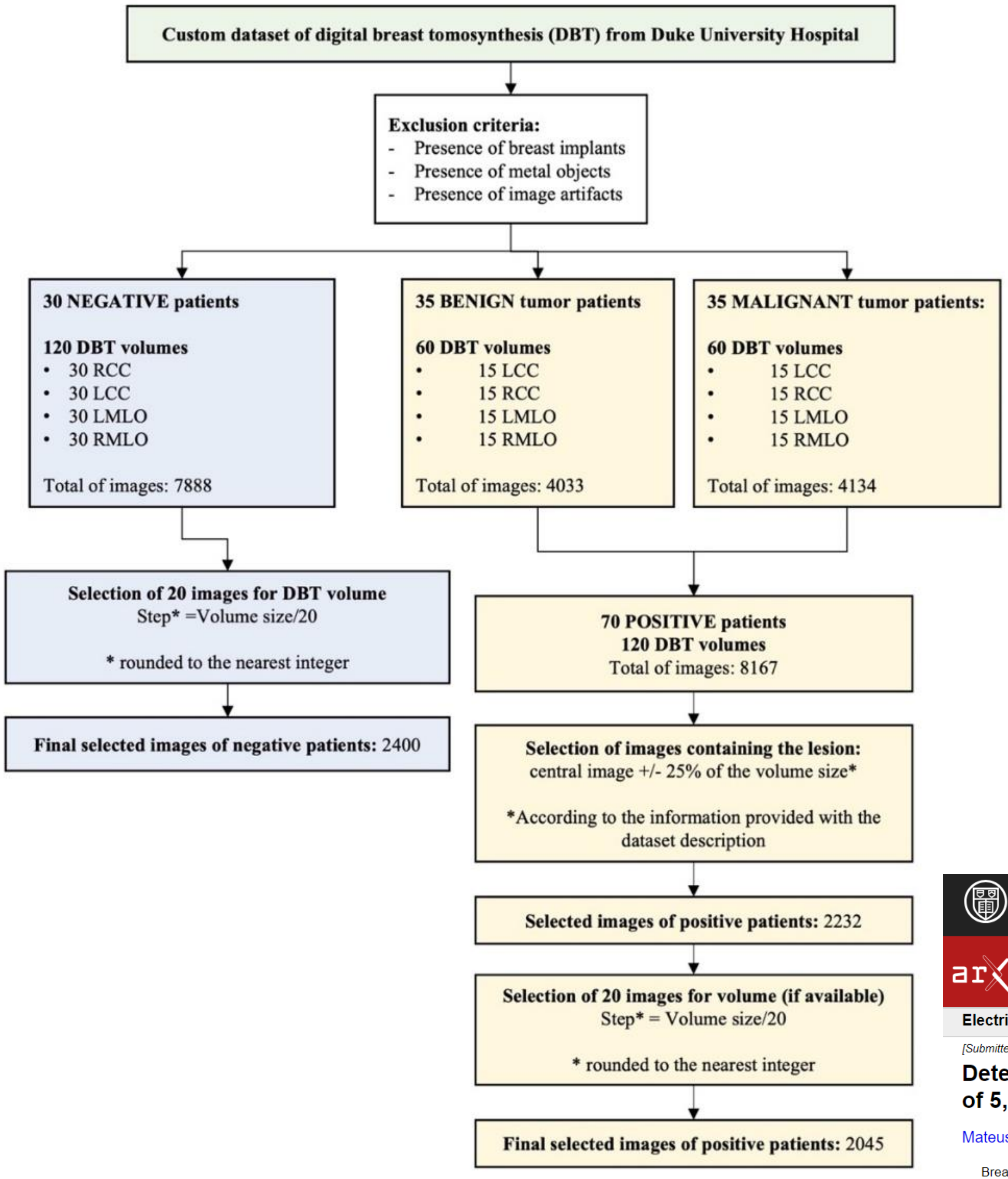

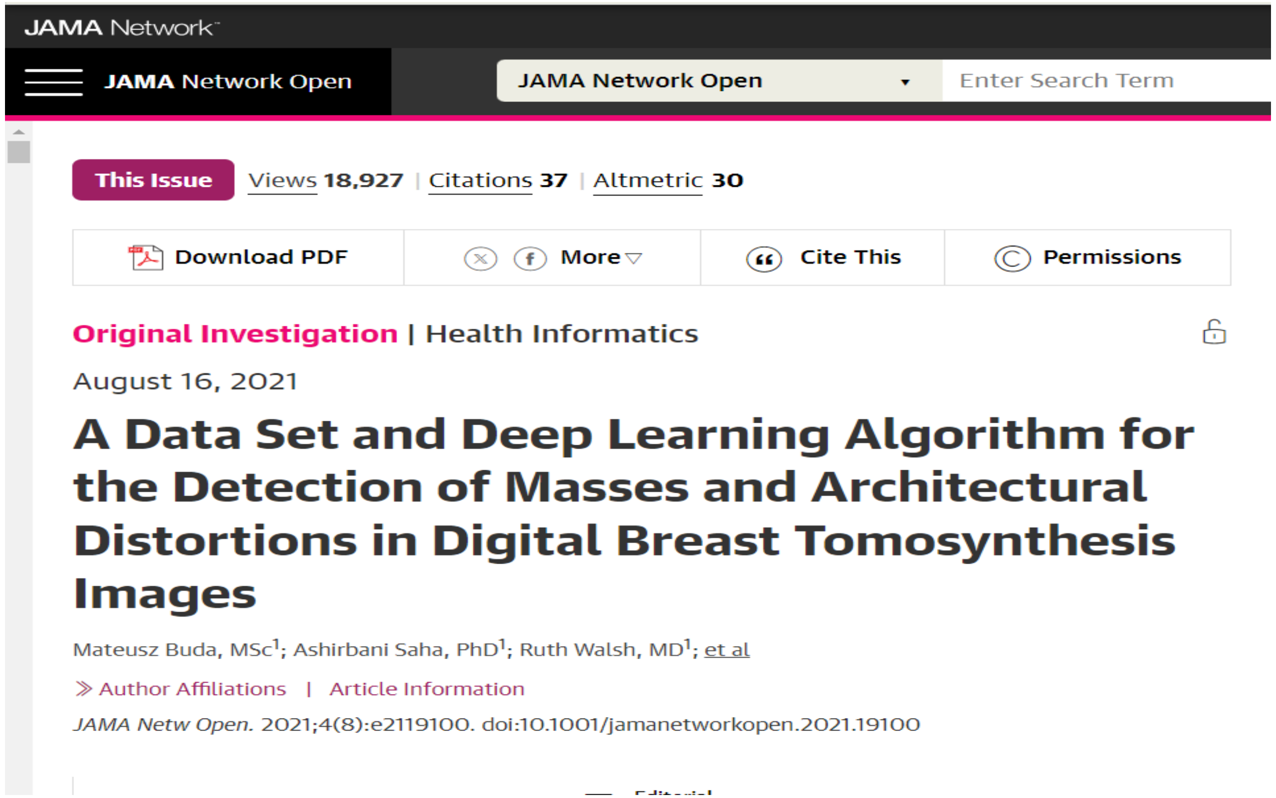

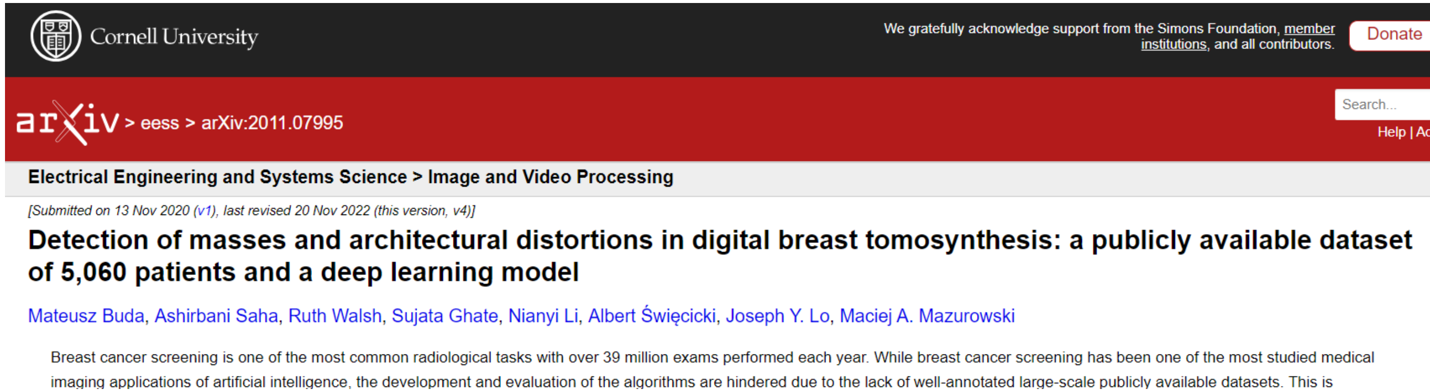

DeepLook pipeline

Step 1

Image
Pre-processing

Preprocessing delle immagini

Importantissimo il lavoro fatto con le GradCAM

PRIMA

Step 1	Riduzione del rumore
Step 2	Incremento del contrasto
Step 3	Eliminazione automatica: • della pelle • del capezzolo • di ulteriori artefatti • del muscolo pettorale ove presente (MLO vista)
Step 4	Binning automatico delle slices a 300 x 300 px

DOPO

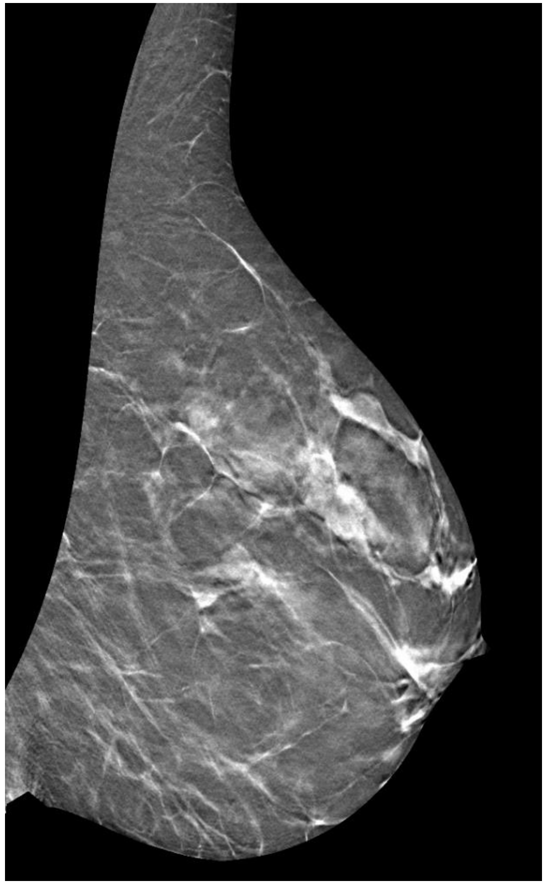

Duke Dataset

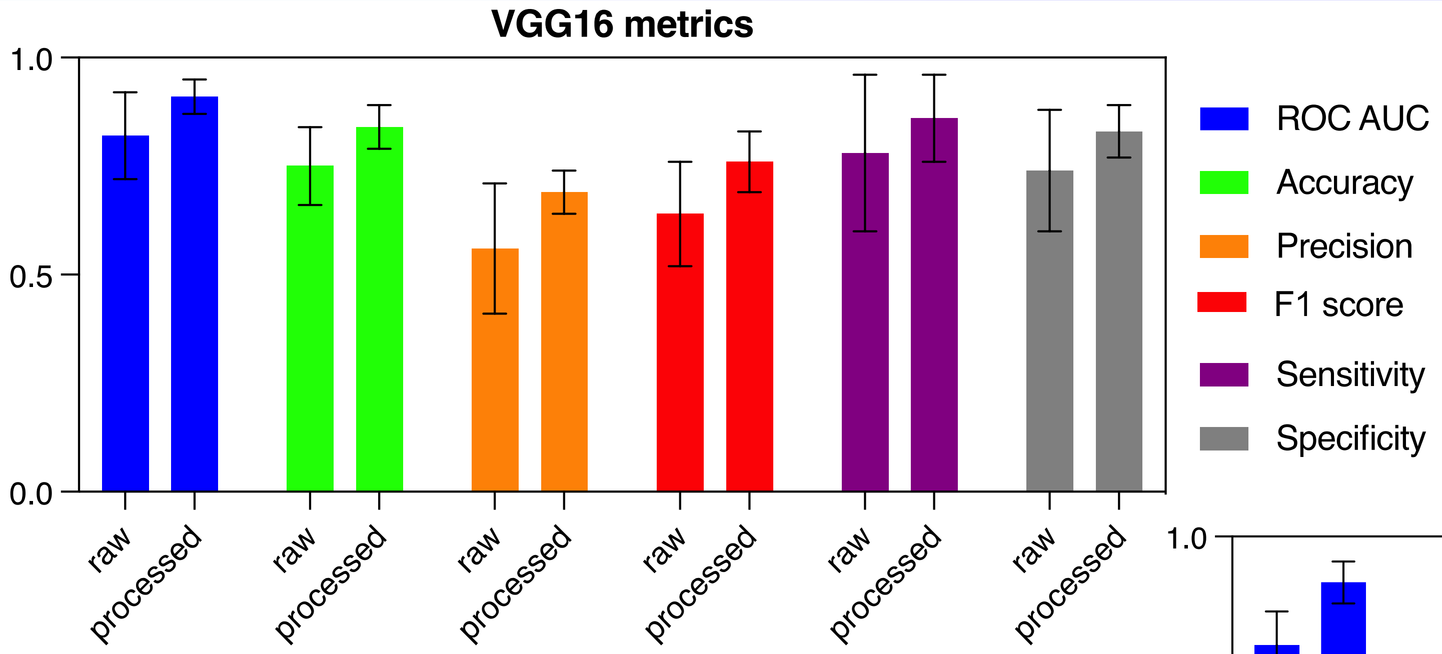

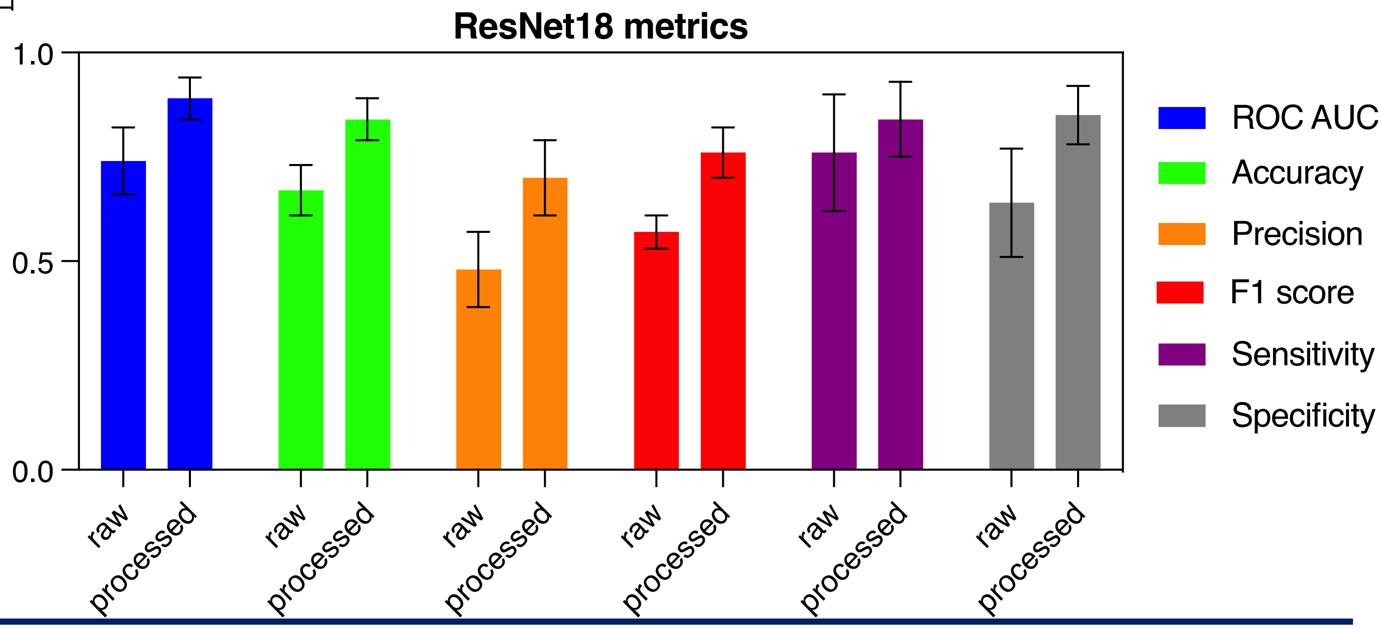

Classification procedure

Step 1

Image
Pre-processing

Step 2

Slice
selection

Slice selection - network

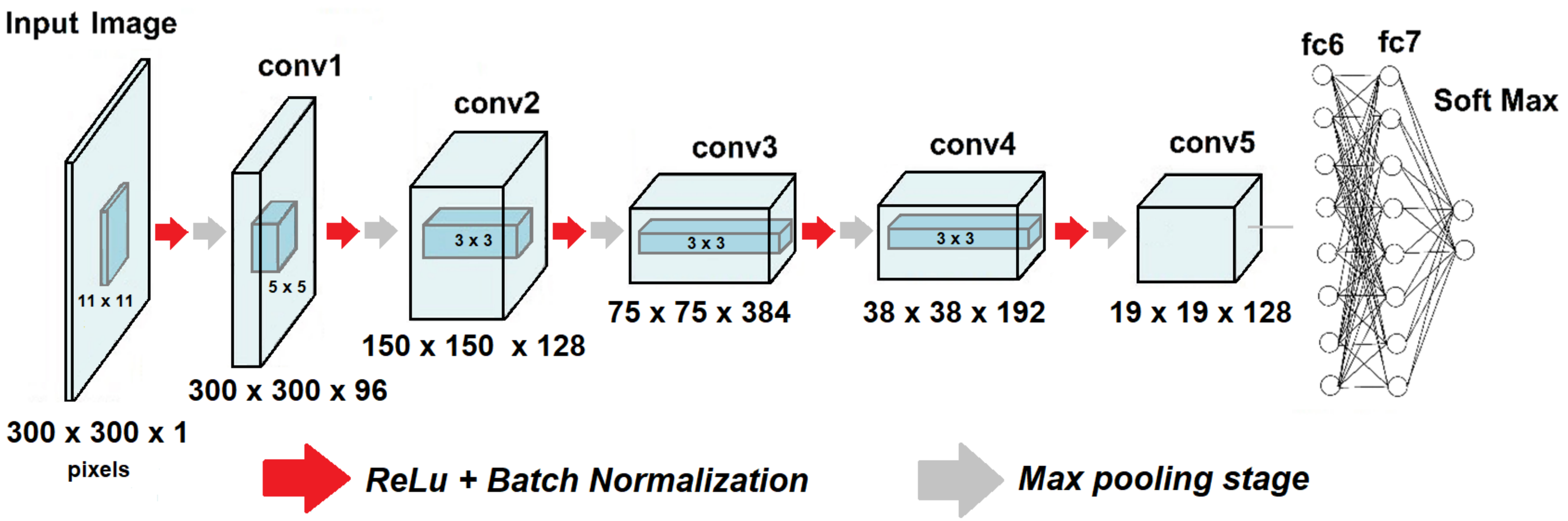

The DCNN-DBT was trained on a GPU NVIDIA GeForce RTX 3090 card (10496 CUDA cores, 24 GB GDDR6X video memory).

Slice selection

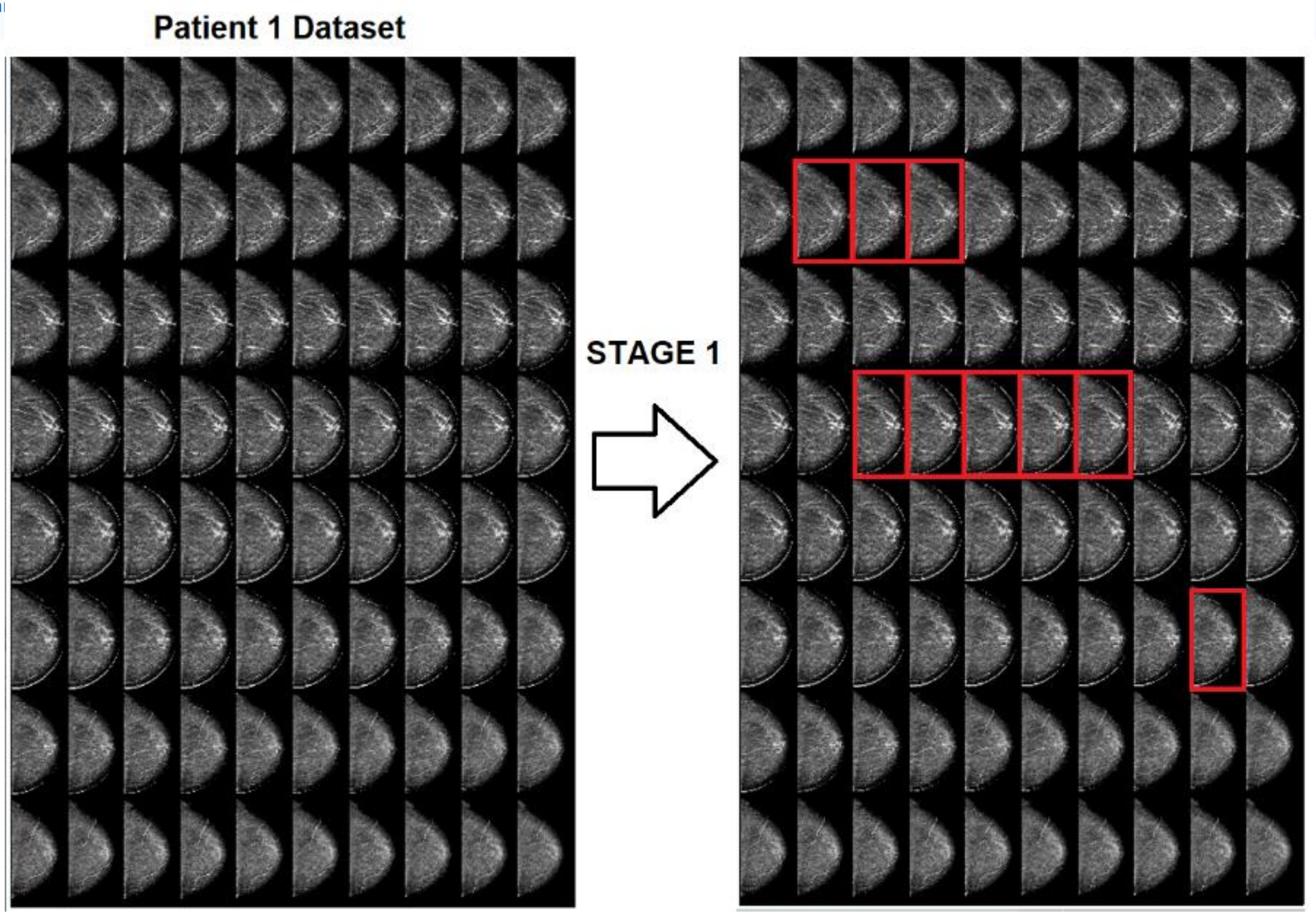

Metrics – Full Dataset

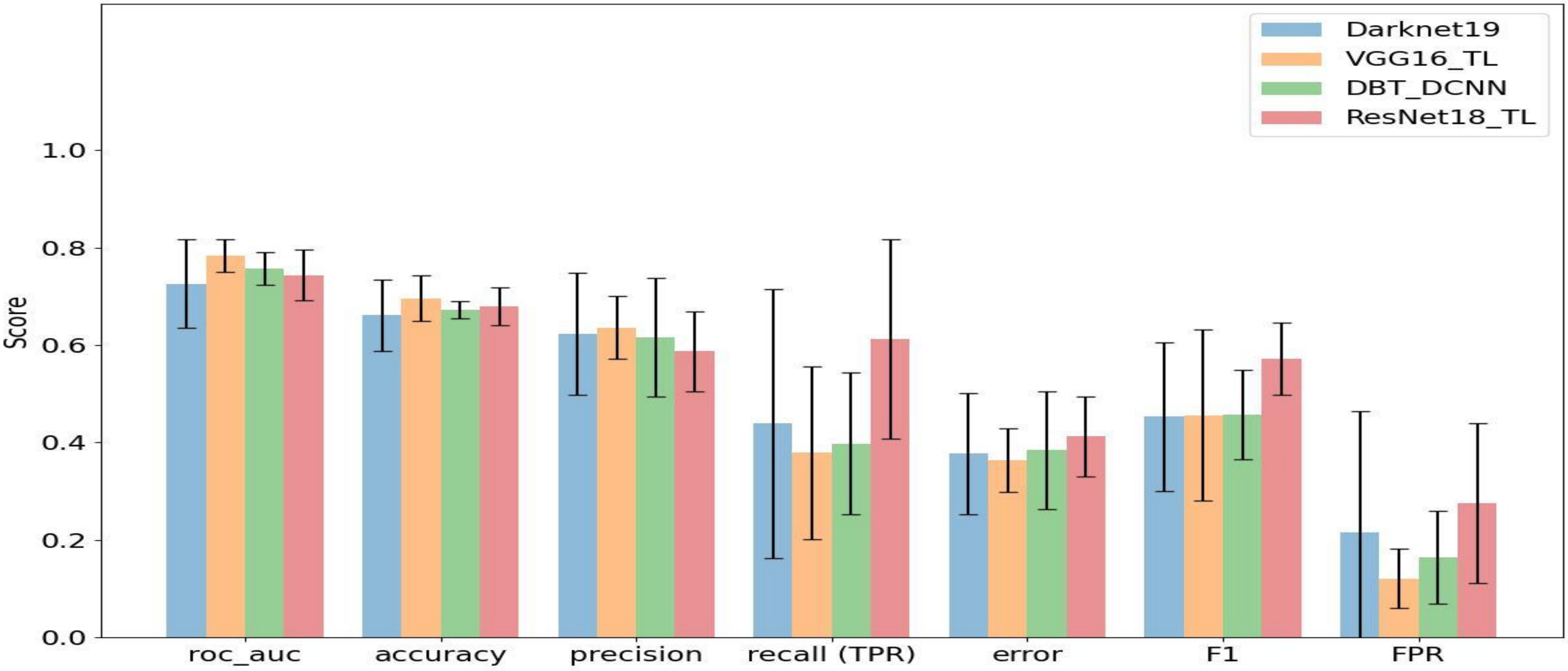

Metrics – Duke Dataset

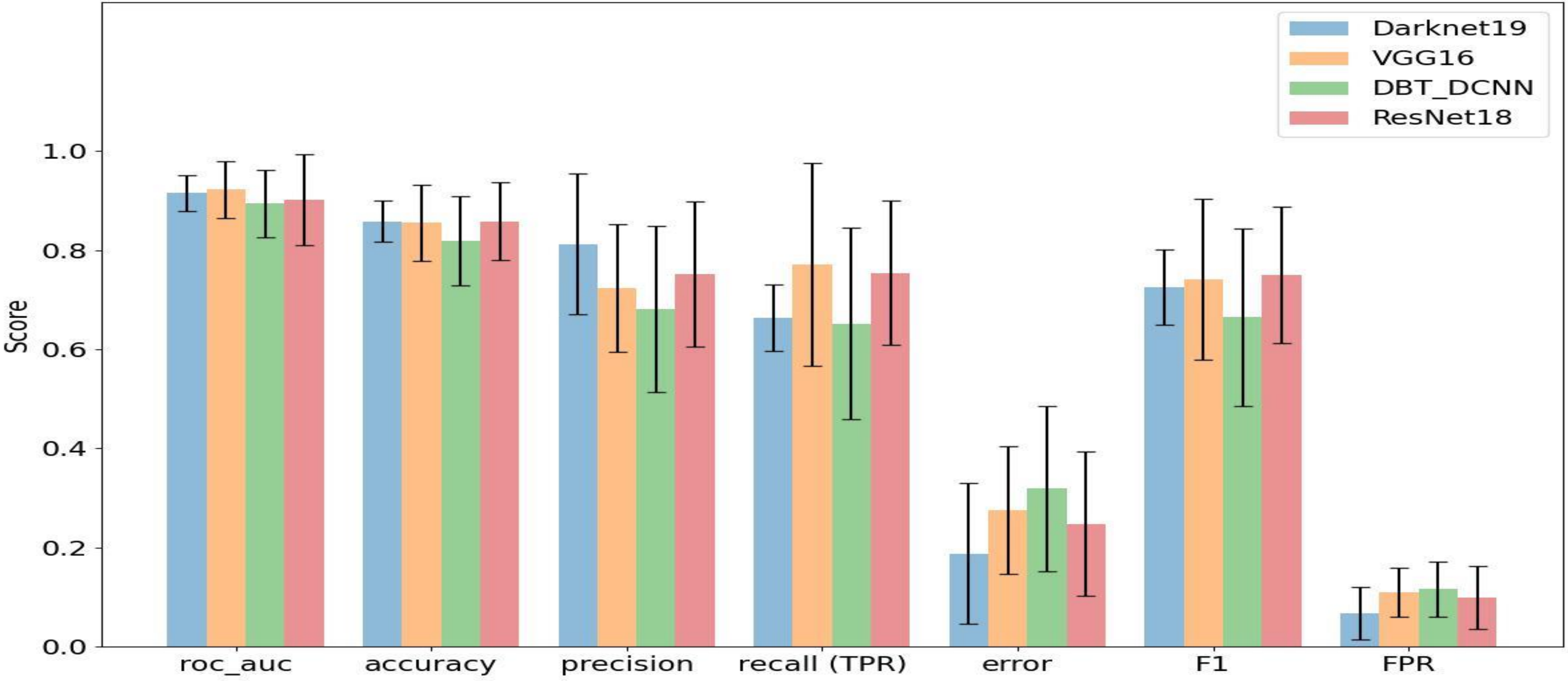

Metrics – Cardarelli Dataset

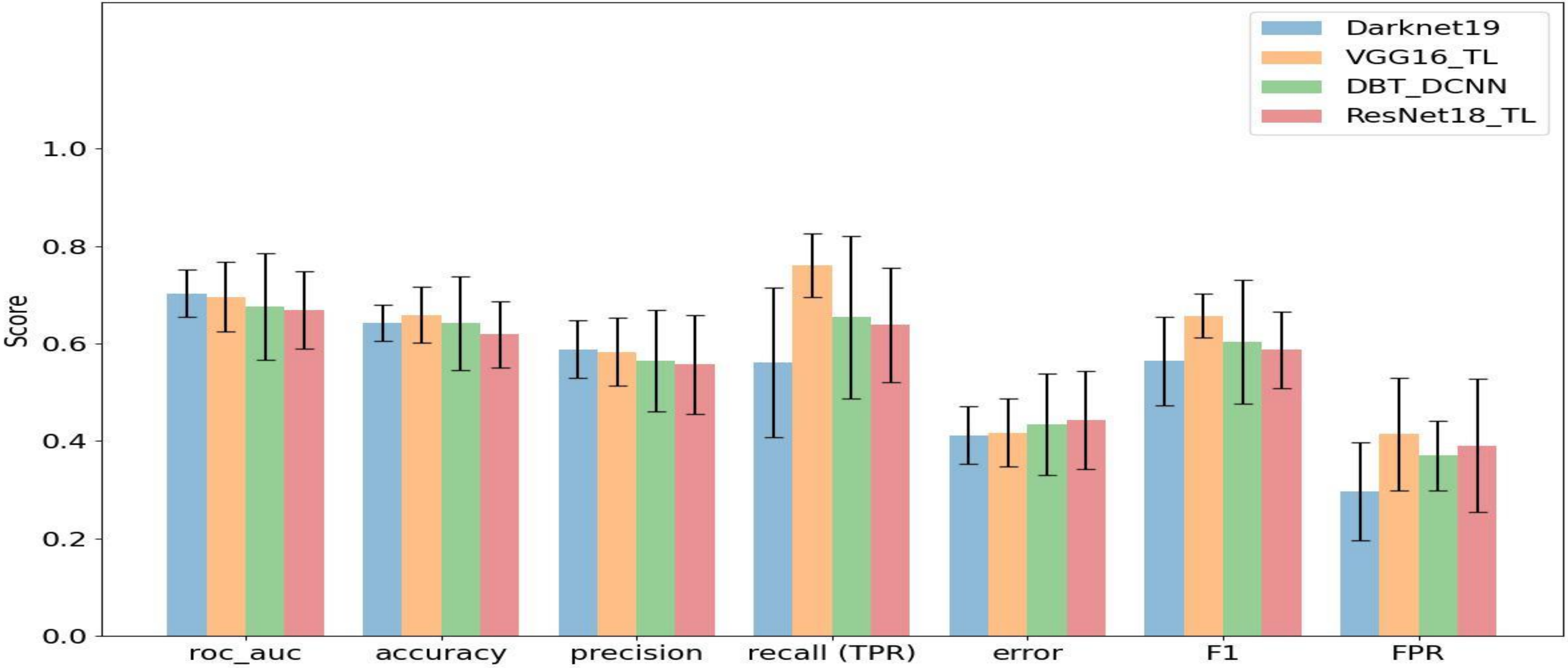

Metrics – IFO Dataset

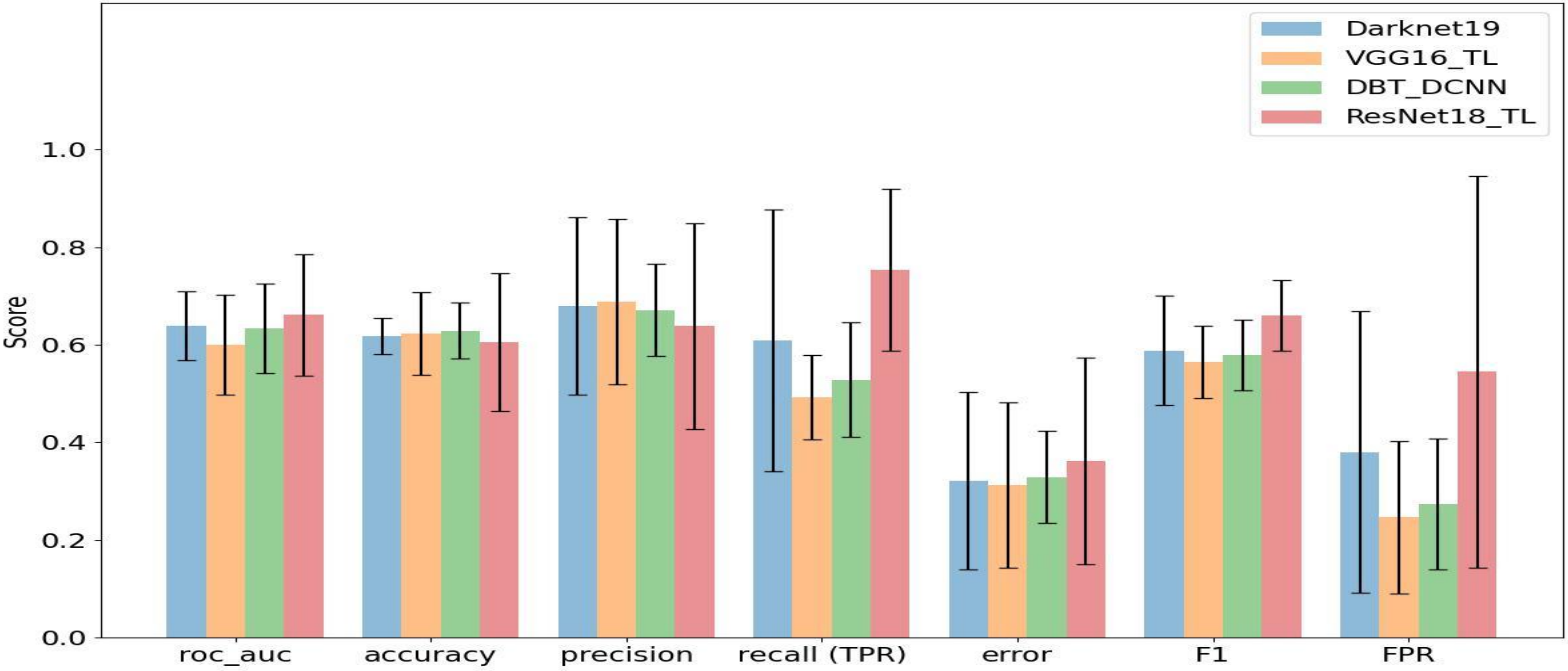

Metrics – 3 Classi

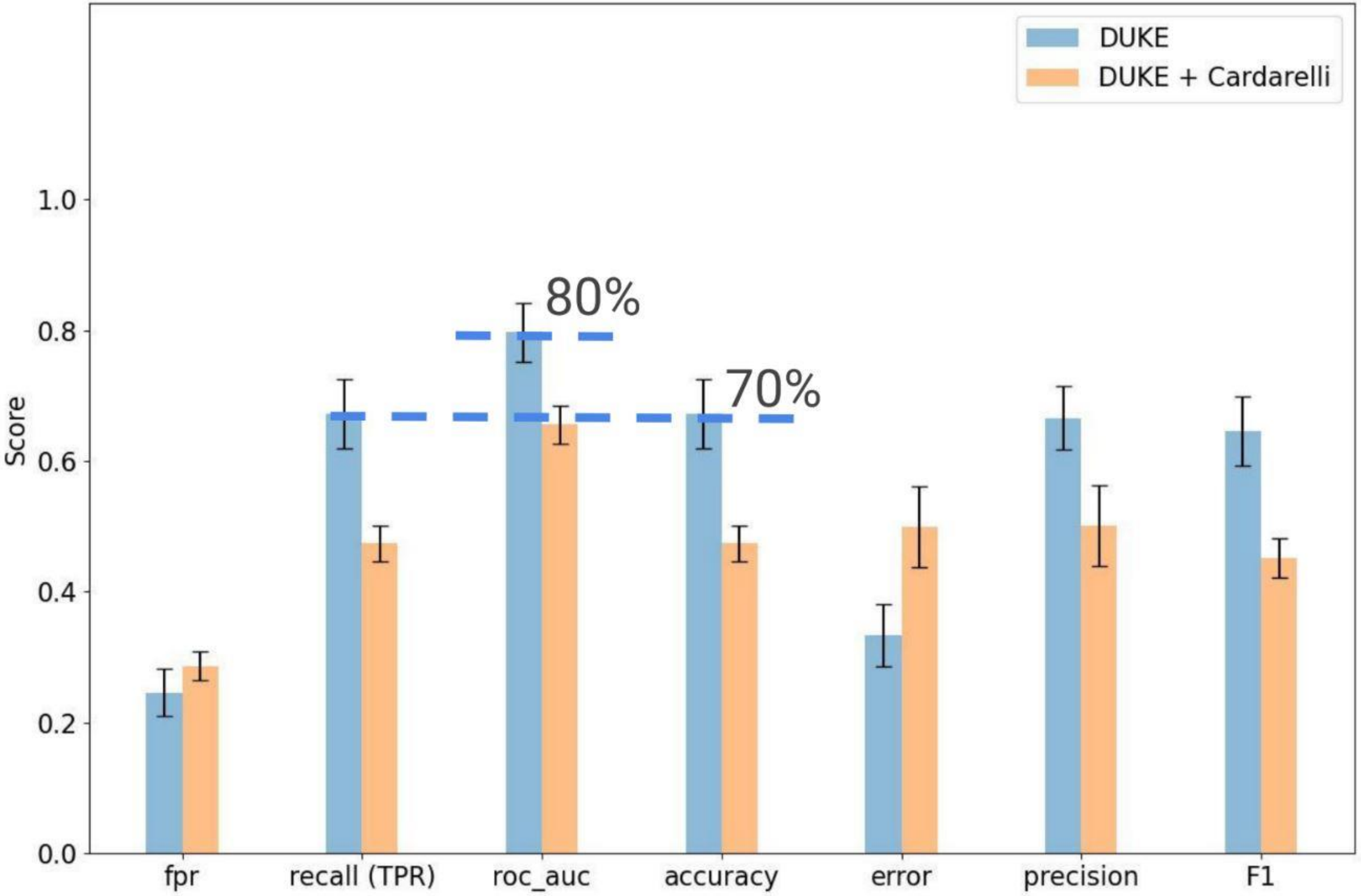

- Negative
- Benign masses
- Malignant masses

Classification procedure

Step 1

Image Pre-processing

Step 2

Slice selection

Step 3

Mass localization

Mass Localization

In this stage, for each identified slices is generated a Grad-CAM map to localize the maximum activation zone and consequently the possible localization of the mass with the definition of a Region of Interest (ROI).

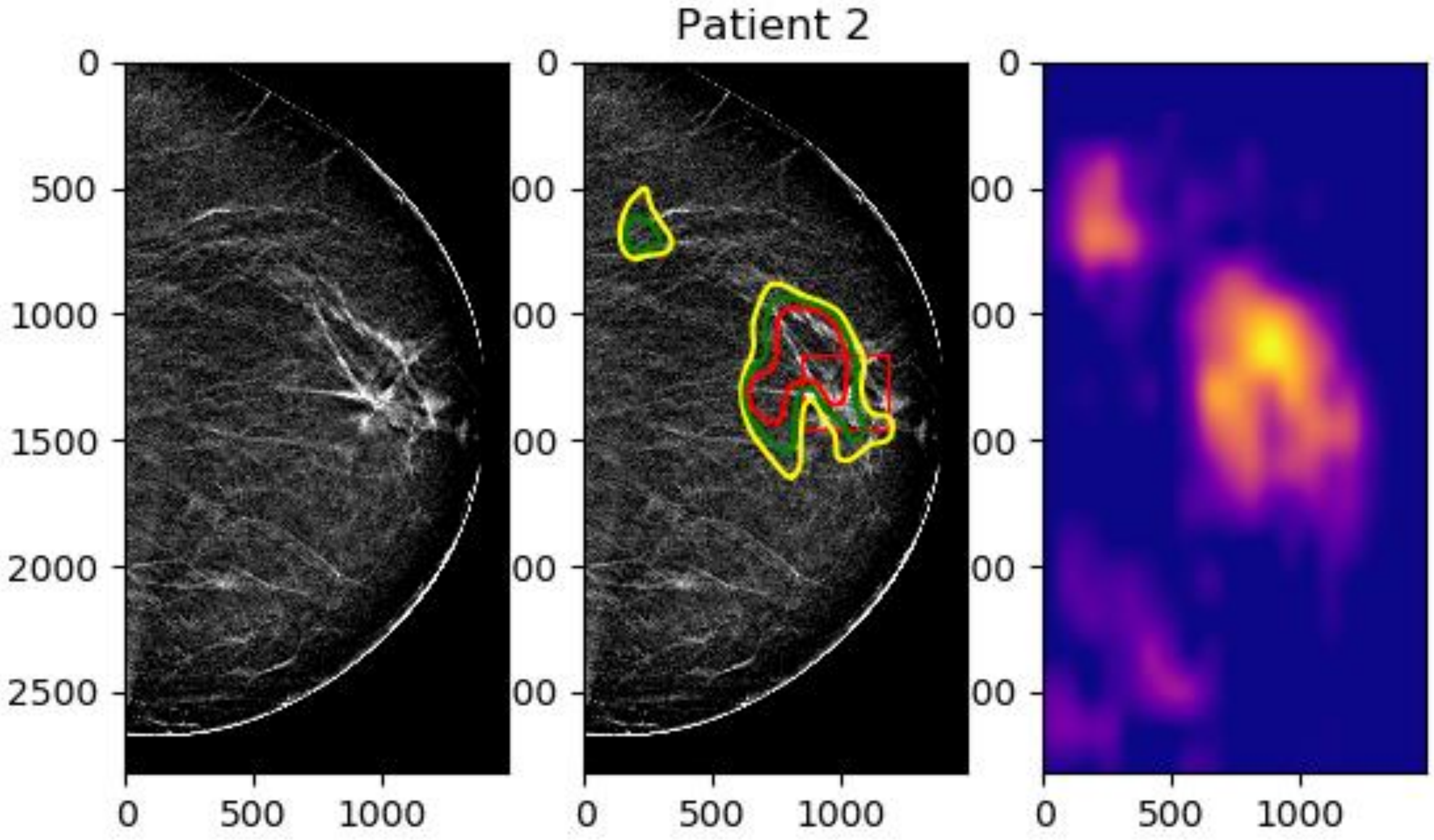

Yellow threshold level of 50%
Green threshold level 60%
Red threshold level 70%

Mass Localization

$$Overlap = \frac{GradCAM\ ROI\ \cap Ground\ Thruh}{Ground\ Thruh};$$

The ratio between the intersection of area of GradCAM ROI and the area indicated by the radiologist.

$$Activation = \frac{GradCAM\ ROI\ dim}{Image\ dim}$$

The ratio between the dimensions of GradCAM ROI and slice.

Mass Localization

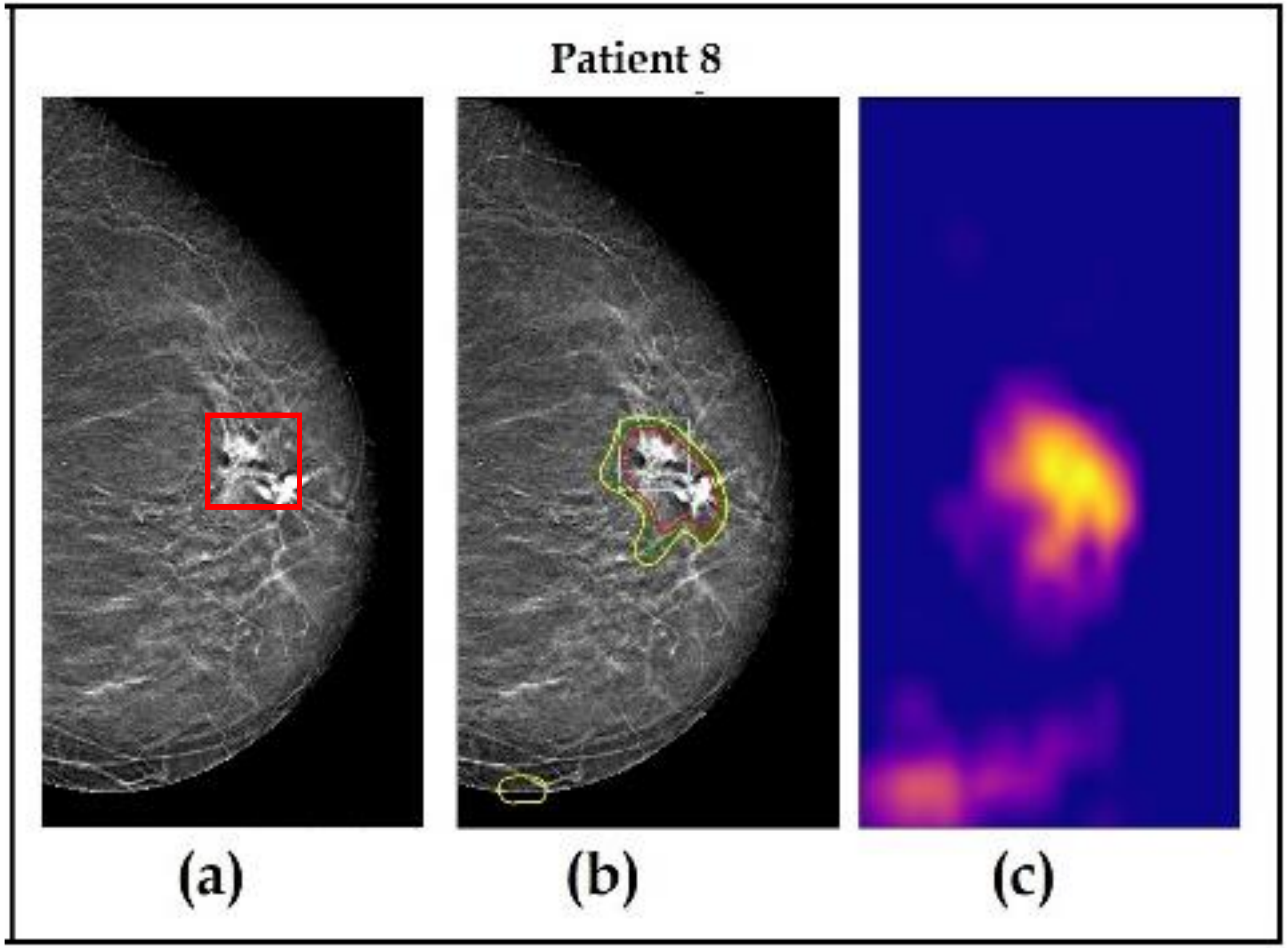

Threshold > 0.5

Overlap = 95%

Activation = 15%

Threshold > 0.6

Overlap = 93%

Activation = 10%

Threshold > 0.7

Overlap = 90%

Activation = 8%

Mass Localization

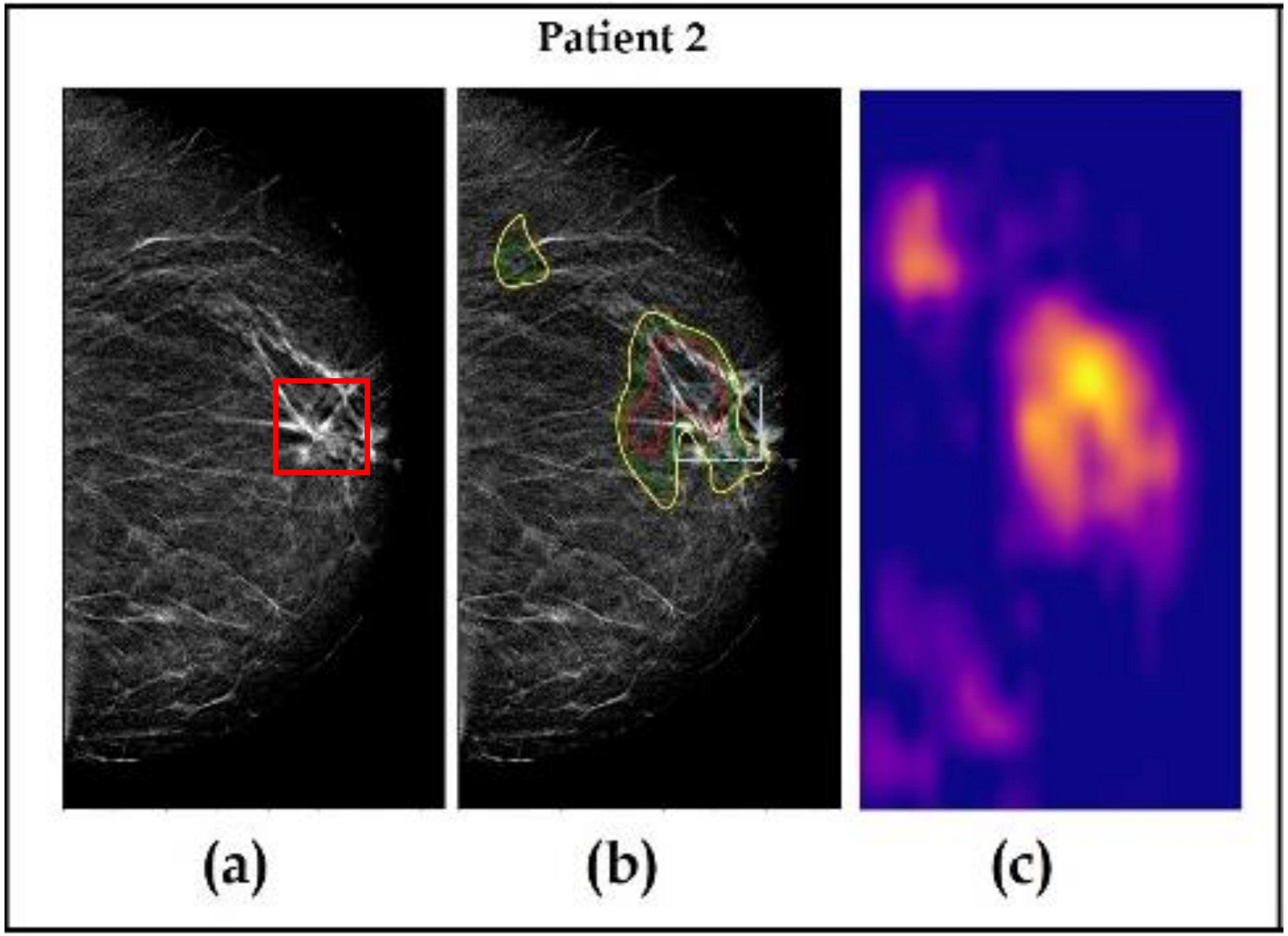

Threshold > 0.5

Overlap = 75%

Activation = 25%

Threshold > 0.6

Overlap = 60%

Activation = 15%

Threshold > 0.7

Overlap = 45%

Activation = 10%

False positive reduction

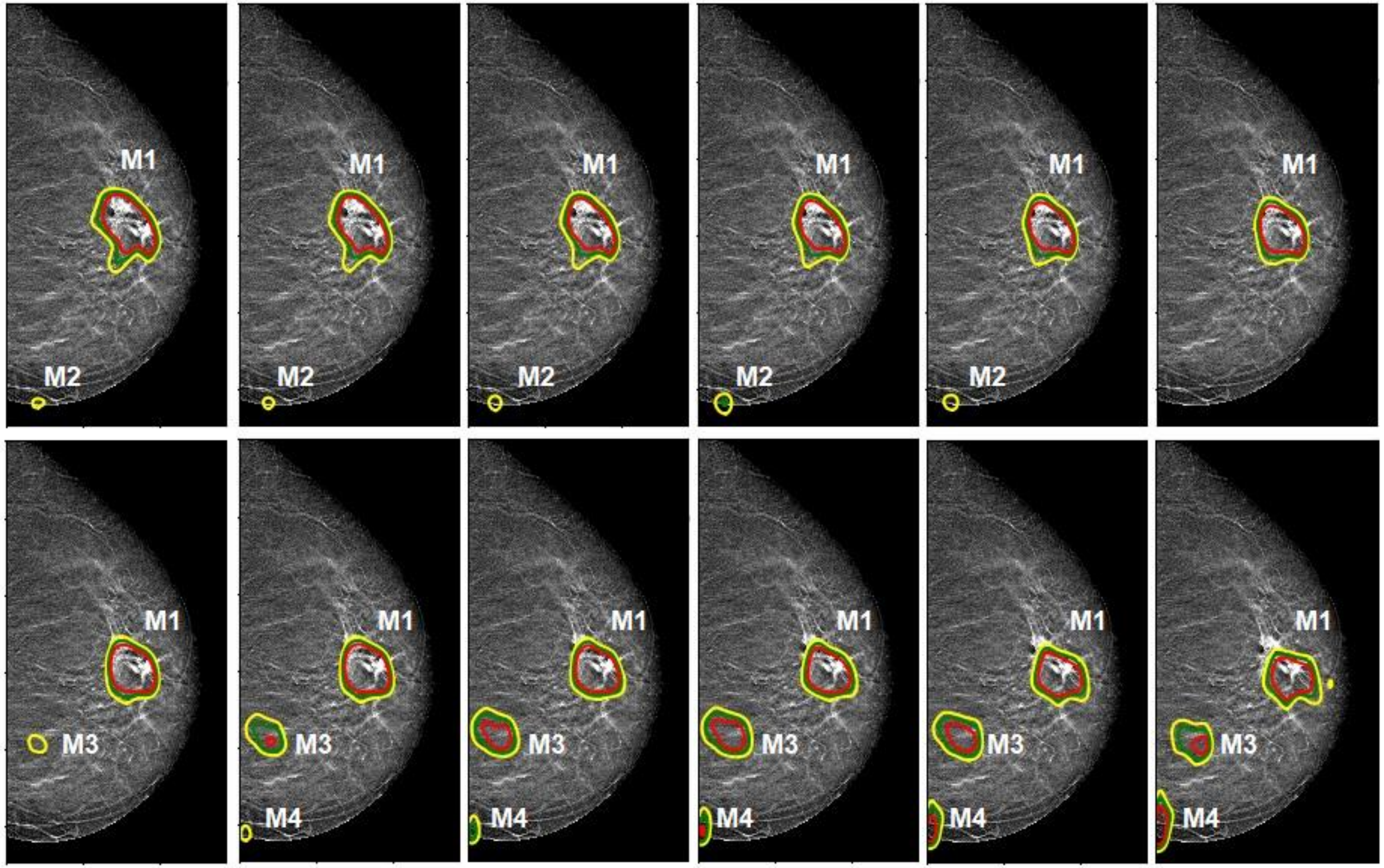

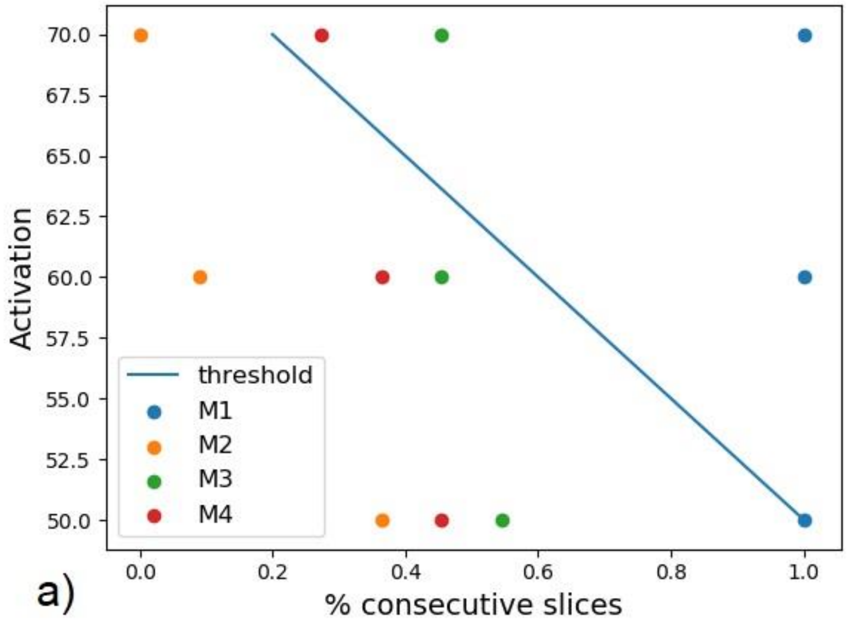

Final result

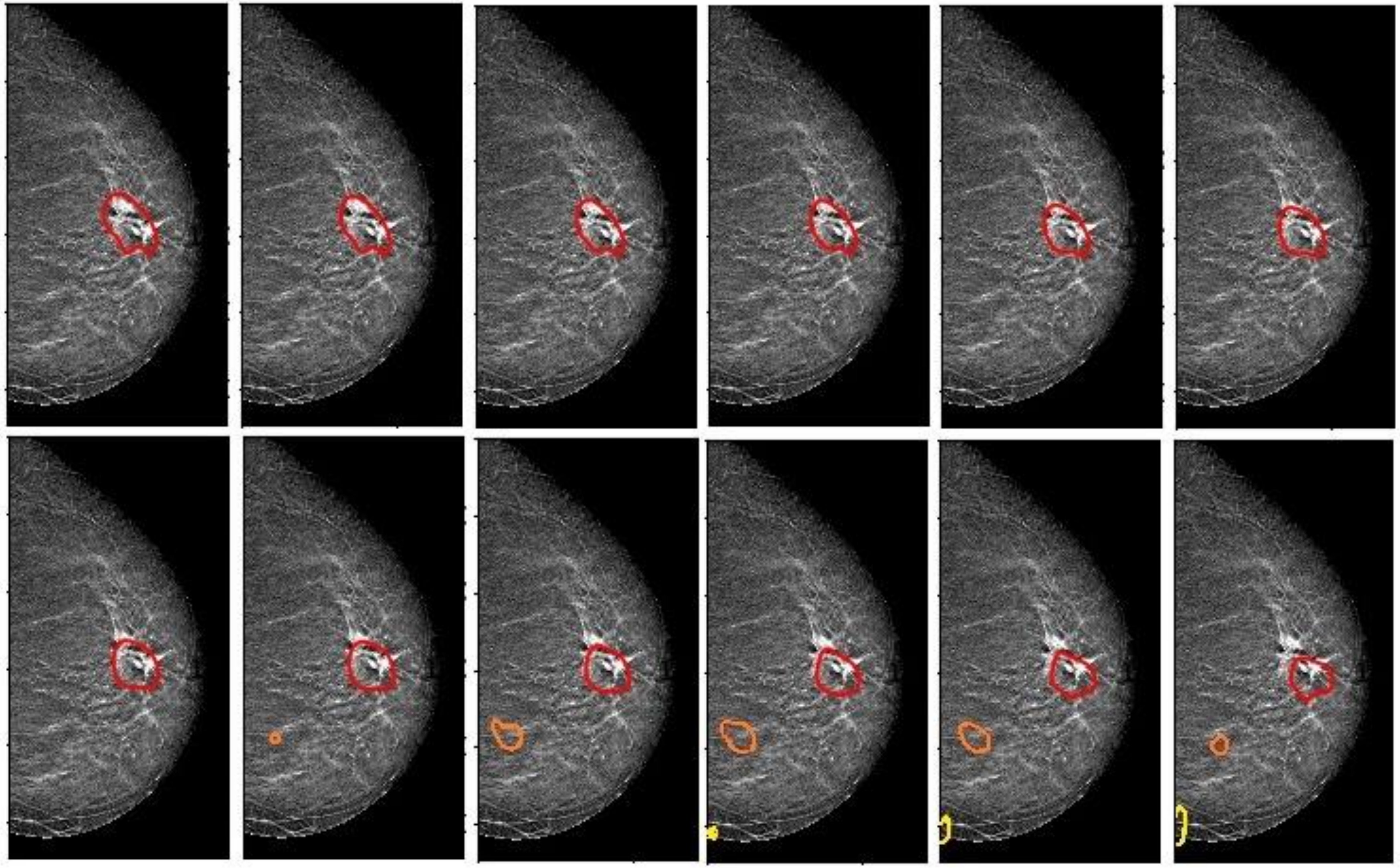

Confidence Level
- Low
- Medium
- High

Classification procedure

Step 1	Step 2	Step 3	Step 4
Image Pre-processing	Slice selection	Mass localization	False positive reduction

Radiomics Module

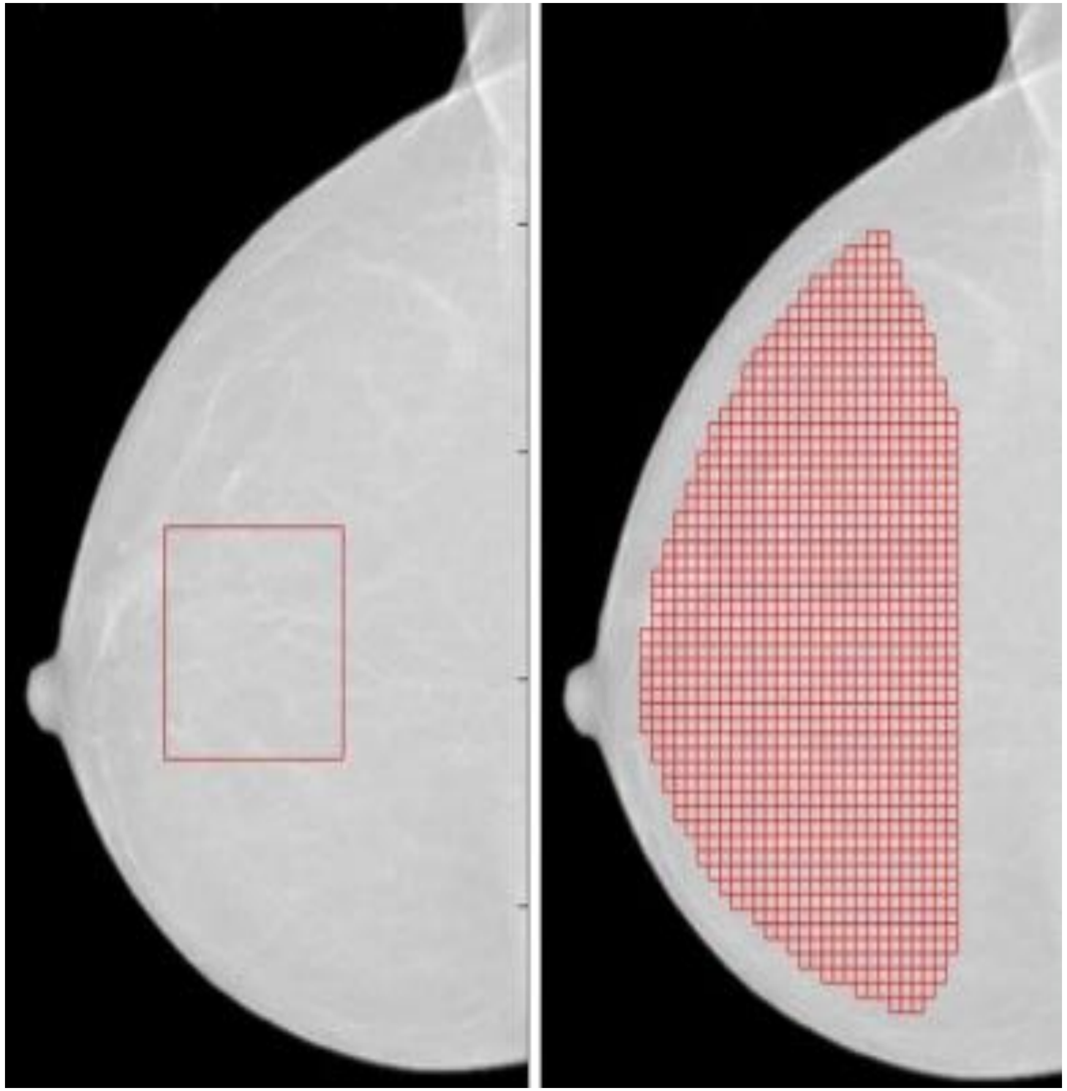

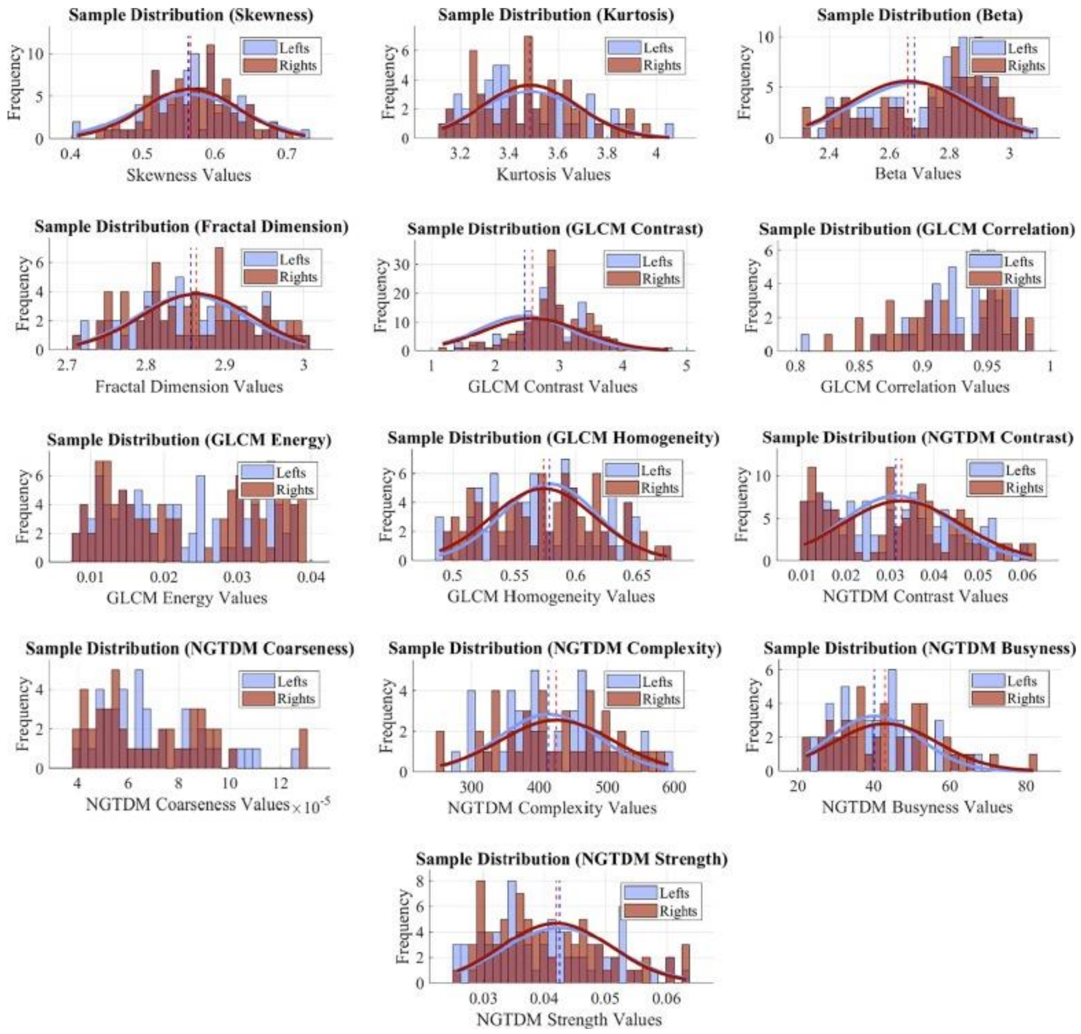

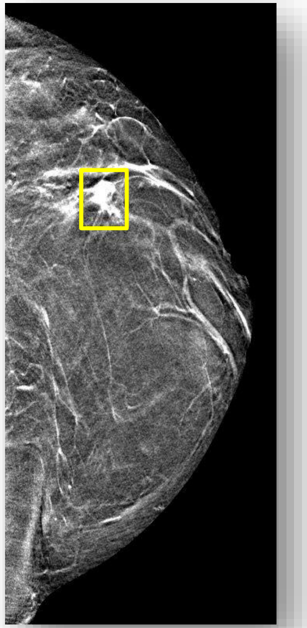

Image Segmentation

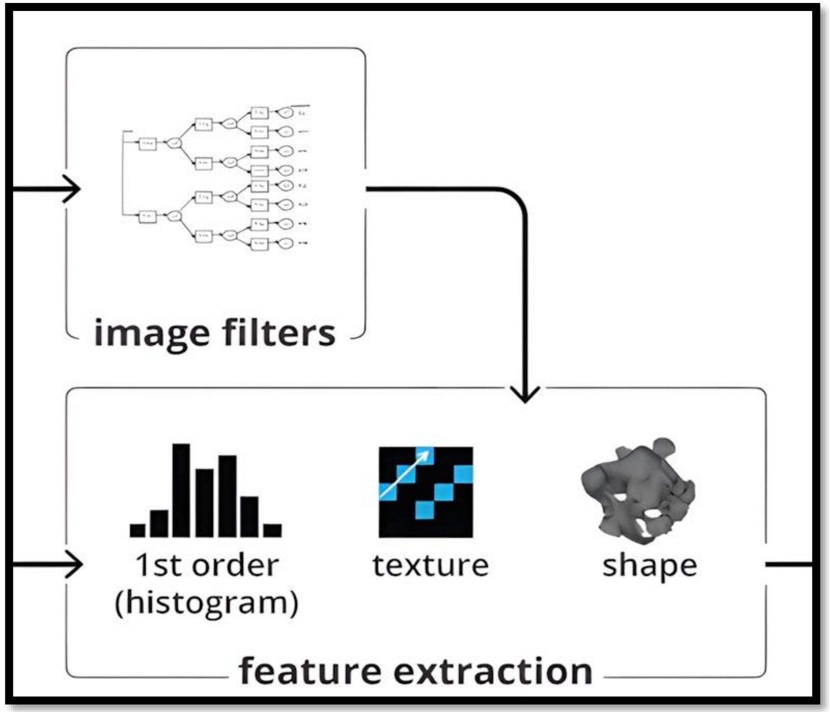

PyRadiomics

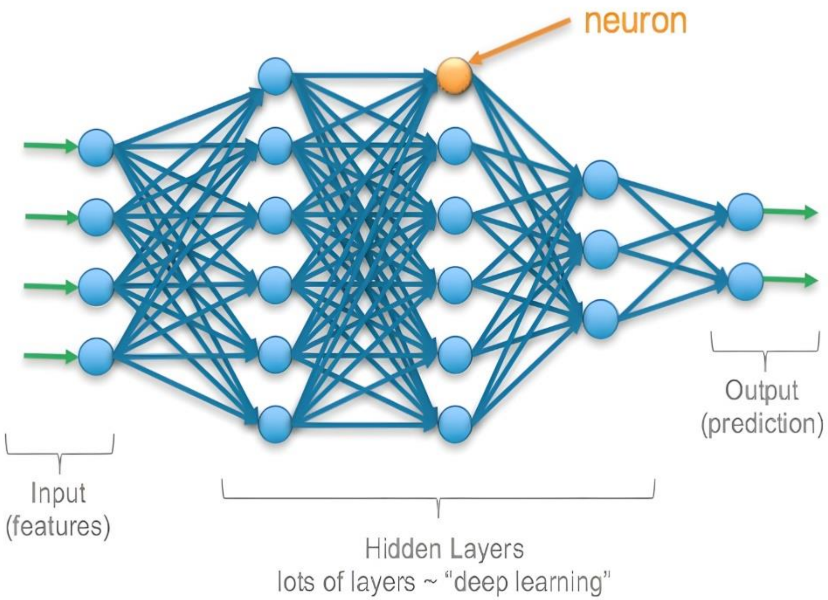

TabNet

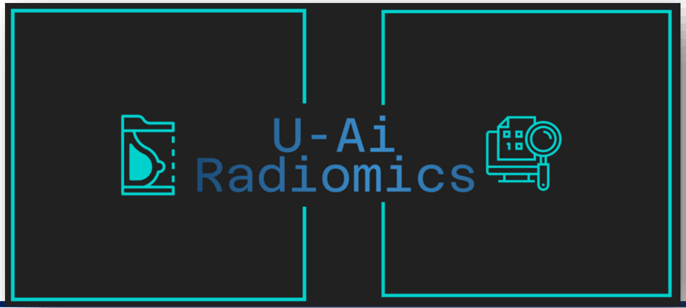

U-Ai Radiomics Parameters Settings Tab

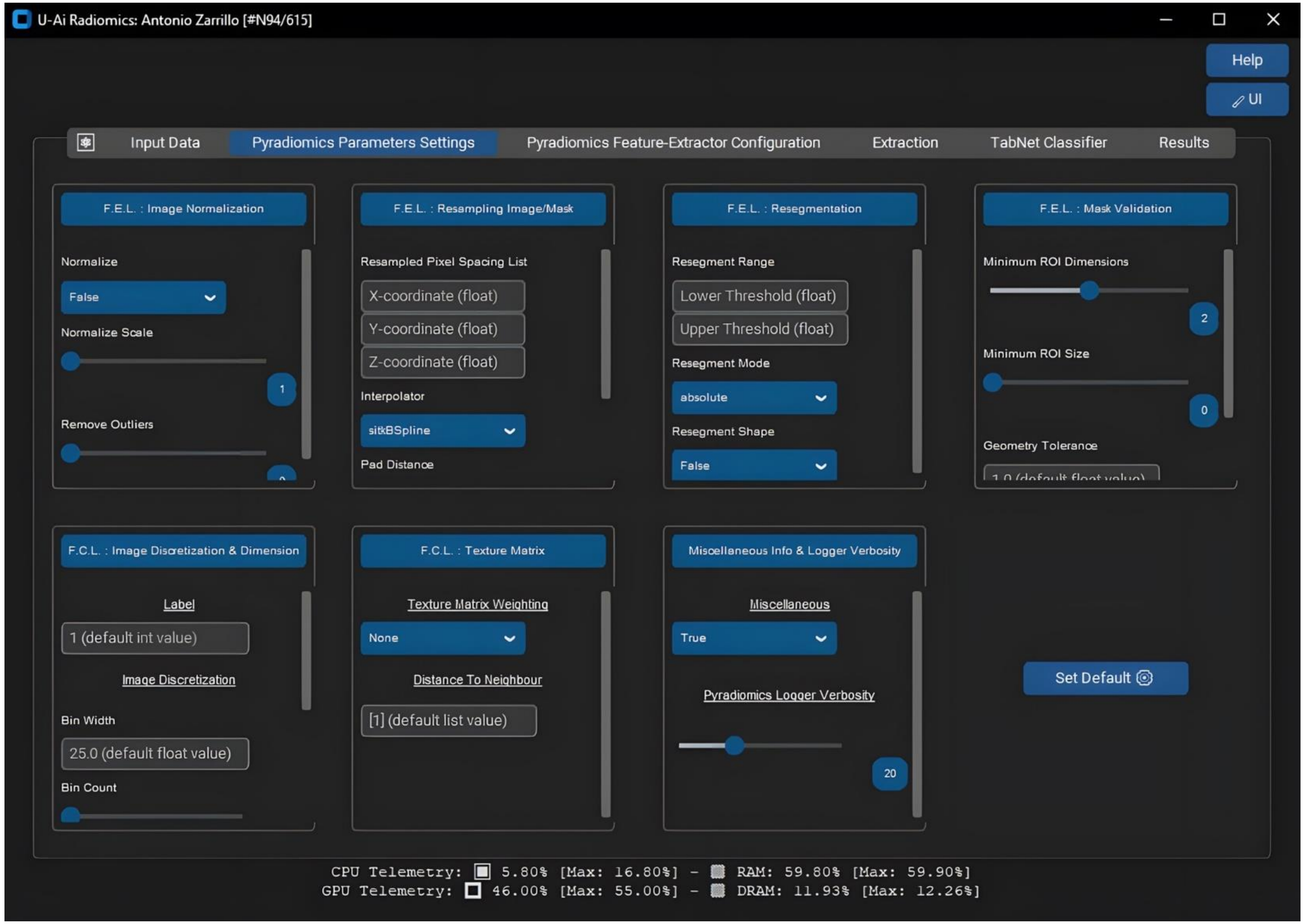

La ***PyRadiomics Parameters Settings Tab*** consente di configurare i parametri di estrazione di PyRadiomics, distinguiamo tre livelli di settings:

- **Feature Extractor Level (F.E.L.)**, per la pre-elaborazione delle immagini e della maschera (segmentazione);
- **Feature Class Level (F.C.L.)**, per la configurazione dei parametri del modulo *feature-extractor*;
- **Miscellaneous Info & Logger Verbosity**, per corredare l'estrazione di informazioni di contorno descrittive dei dati di input o del processo di estrazione.

U-Ai Radiomics Features Extractor Configuration Tab

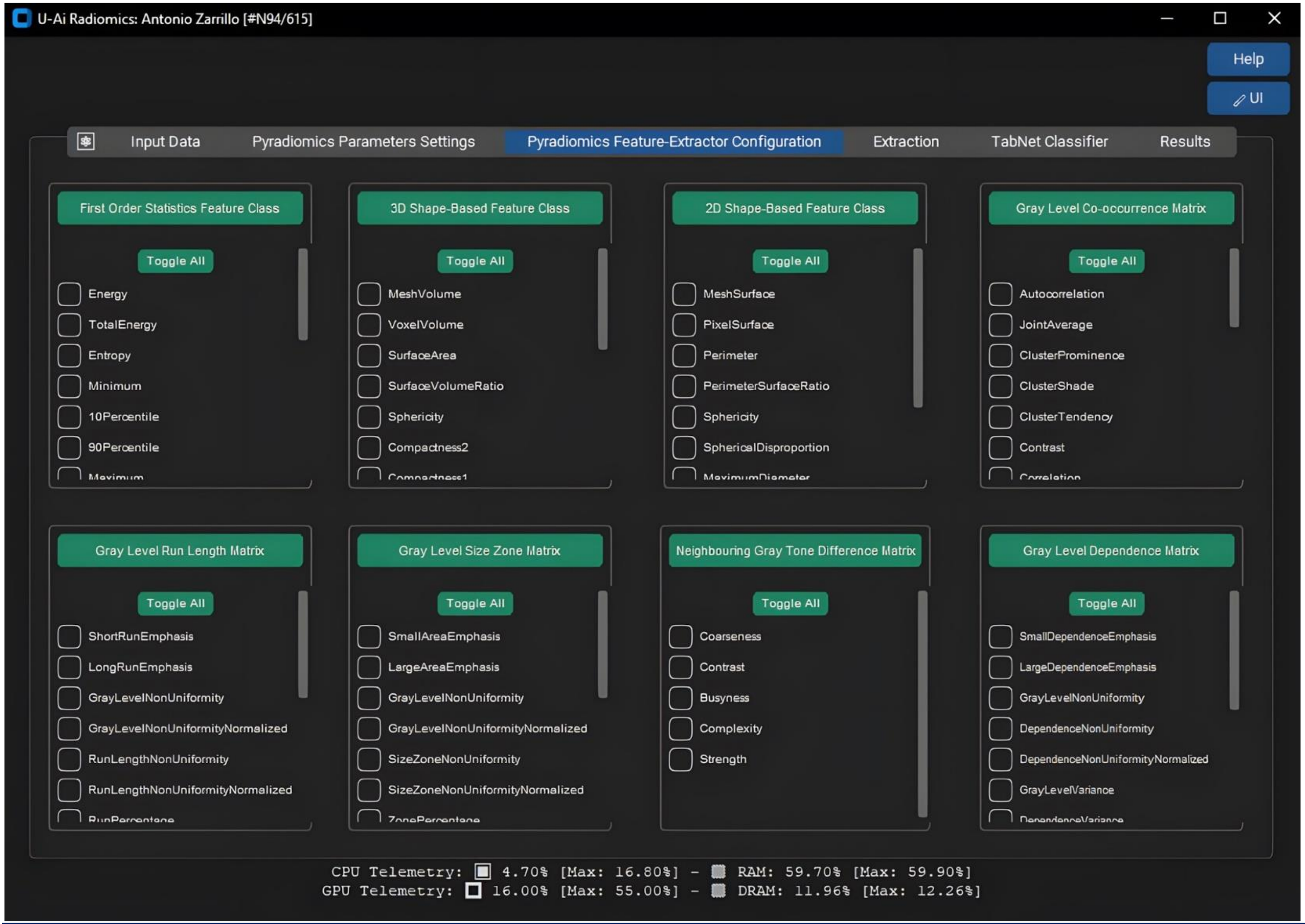

La ***PyRadiomics Features Extractor Configuration Tab*** consente di selezionare manualmente le features che il modulo ferature-extractor andrà a calcolare entro la maschera di segmentazione:

- ***First order statistics -*** *1 classe, 19 features*;
- ***Shape features -*** *2 classi, 27 features*;
- ***Texture features -*** *5 classi, 74 features*.

Totale: 8 classi, 120 features

U-Ai Radiomics Results Tab

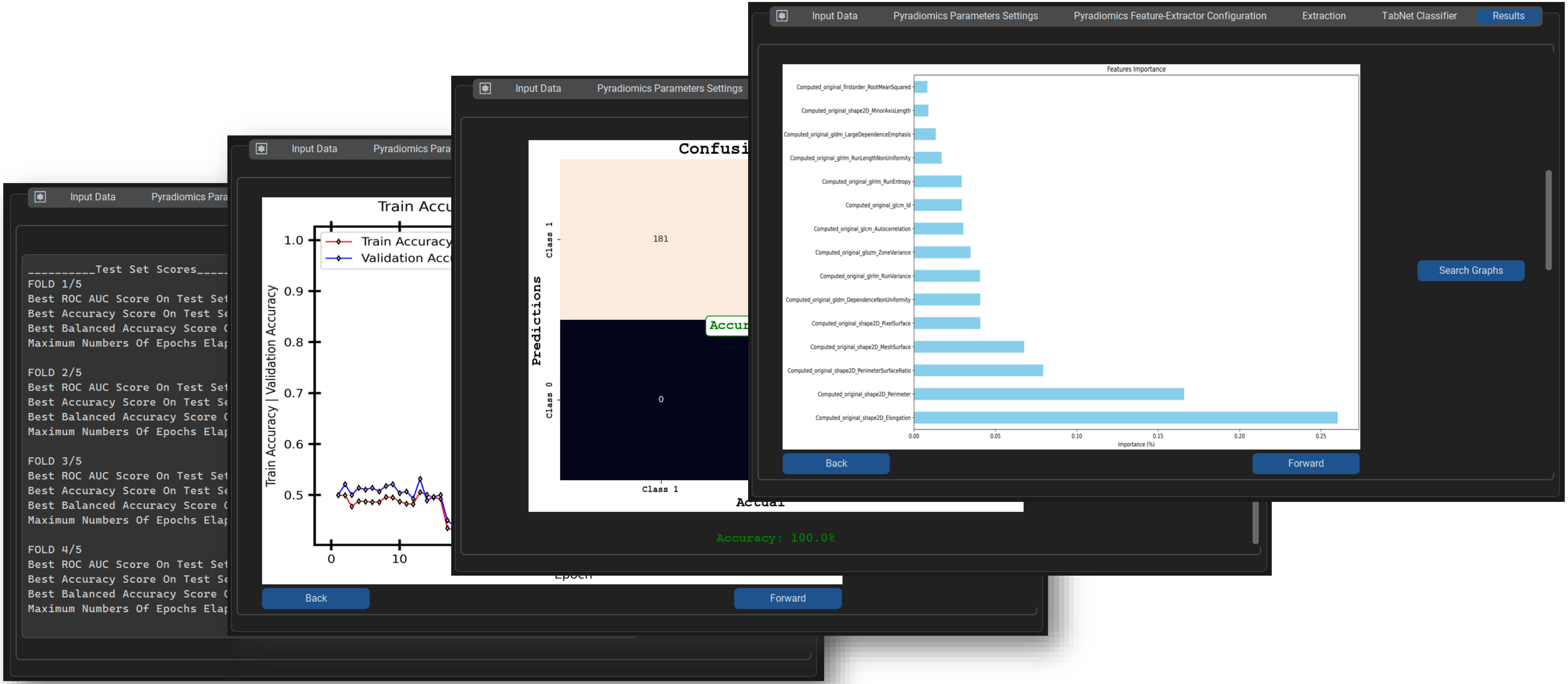

CARD&IFO *(best fold; N$_d$ = 31)*

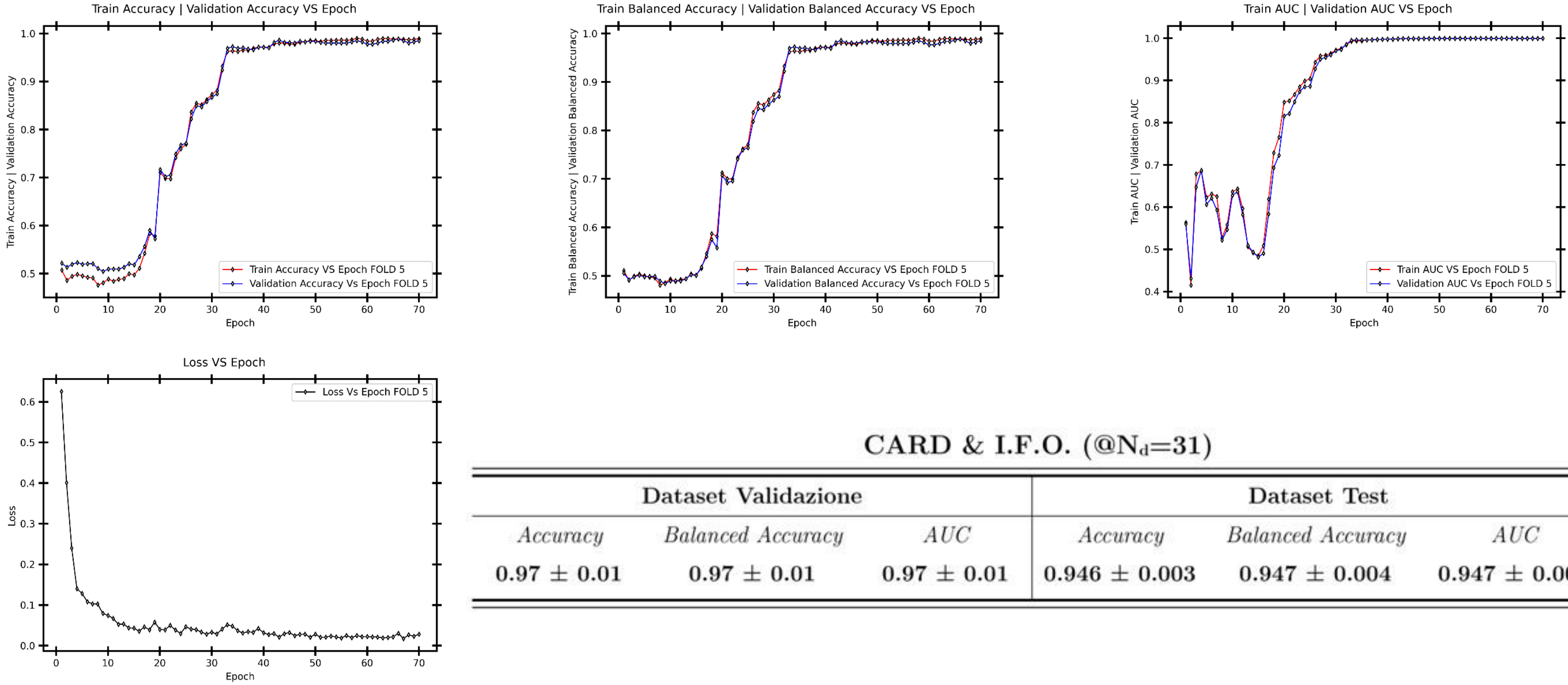

CARD & I.F.O. (@N$_d$=31)

Dataset Validazione			Dataset Test		
Accuracy	*Balanced Accuracy*	*AUC*	*Accuracy*	*Balanced Accuracy*	*AUC*
0.97 ± 0.01	0.97 ± 0.01	0.97 ± 0.01	0.946 ± 0.003	0.947 ± 0.004	0.947 ± 0.004

CARD&IFO (best model's **Folds' Top 5%)**

CARD

Features	Max Folds' Importance (%)
Computed_original_shape2D_MajorAxisLength	22.57
Computed_original_shape2D_Elongation	22.14
Computed_original_shape2D_MeshSurface	17.24
Computed_original_shape2D_MinorAxisLength	14.40
Computed_original_gldm_DependenceNonUniformity	13.15
Computed_original_shape2D_PerimeterSurfaceRatio	11.55
Computed_original_shape2D_Perimeter	8.50
Computed_original_gldm_DependenceEntropy	8.47
Computed_original_shape2D_PixelSurface	8.40
Computed_original_glcm_ClusterShade	6.06
Computed_original_glszm_SizeZoneNonUniformity	5.92
Computed_original_shape2D_MaximumDiameter	5.65

IFO

Features	Max Folds' Importance (%)
Computed_original_shape2D_MaximumDiameter	19.69
Computed_original_shape2D_Elongation	18.65
Computed_original_shape2D_MinorAxisLength	15.25
Computed_original_glrlm_RunLengthNonUniformity	14.84
Computed_original_gldm_HighGrayLevelEmphasis	10.80
Computed_original_shape2D_Perimeter	8.02
Computed_original_shape2D_PerimeterSurfaceRatio	7.67
Computed_original_firstorder_TotalEnergy	6.33
Computed_original_firstorder_10Percentile	5.29
Computed_original_shape2D_MeshSurface	5.03
Computed_original_shape2D_MajorAxisLength	3.69
Computed_original_firstorder_Range	3.63

CARD&IFO **N$_d$** *= 48 Vs* **SK=OFF**
(best model's **Folds' Top 5%)**

Features	Max Folds' Importance (%)
Computed_original_shape2D_MinorAxisLength	17.12
Computed_original_shape2D_Elongation	16.63
Computed_original_shape2D_MajorAxisLength	12.13
Computed_original_shape2D_MaximumDiameter	10.52
Computed_original_gldm_DependenceNonUniformity	9.45
Computed_original_glszm_SizeZoneNonUniformity	9.23
Computed_original_shape2D_Perimeter	8.47
Computed_original_shape2D_PerimeterSurfaceRatio	7.23
Computed_original_shape2D_MeshSurface	7.11
Computed_original_glrlm_RunLengthNonUniformity	6.87
Computed_original_firstorder_Energy	5.28
Computed_original_shape2D_PixelSurface	4.92
Computed_original_glcm_Correlation	4.61
Computed_original_glcm_ClusterShade	4.23
Computed_original_glcm_MCC	3.63
Computed_original_firstorder_Skewness	3.60
Computed_original_glcm_Autocorrelation	3.51
Computed_original_ngtdm_Strength	3.46
Computed_original_firstorder_Range	3.28
Computed_original_firstorder_TotalEnergy	3.20
Computed_original_gldm_DependenceNonUniformityNormalized	3.20
Computed_original_firstorder_Variance	3.04
Computed_original_ngtdm_Complexity	2.87
Computed_original_glszm_SmallAreaLowGrayLevelEmphasis	2.87

CARD & IFO

Super Resolution Neural Network

Original (118x124)

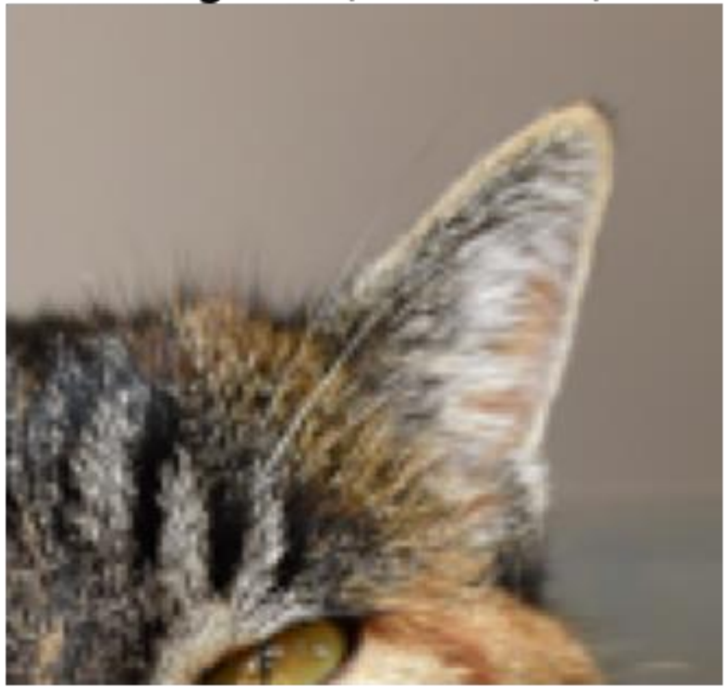

EDSR (472x496)

SRGAN (472x496)

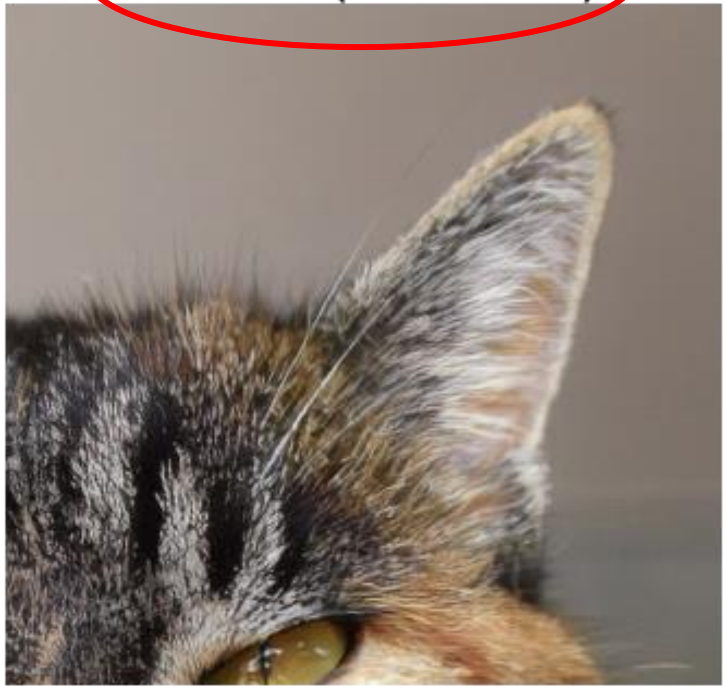

Super Resolution workflow

GAN model architecture

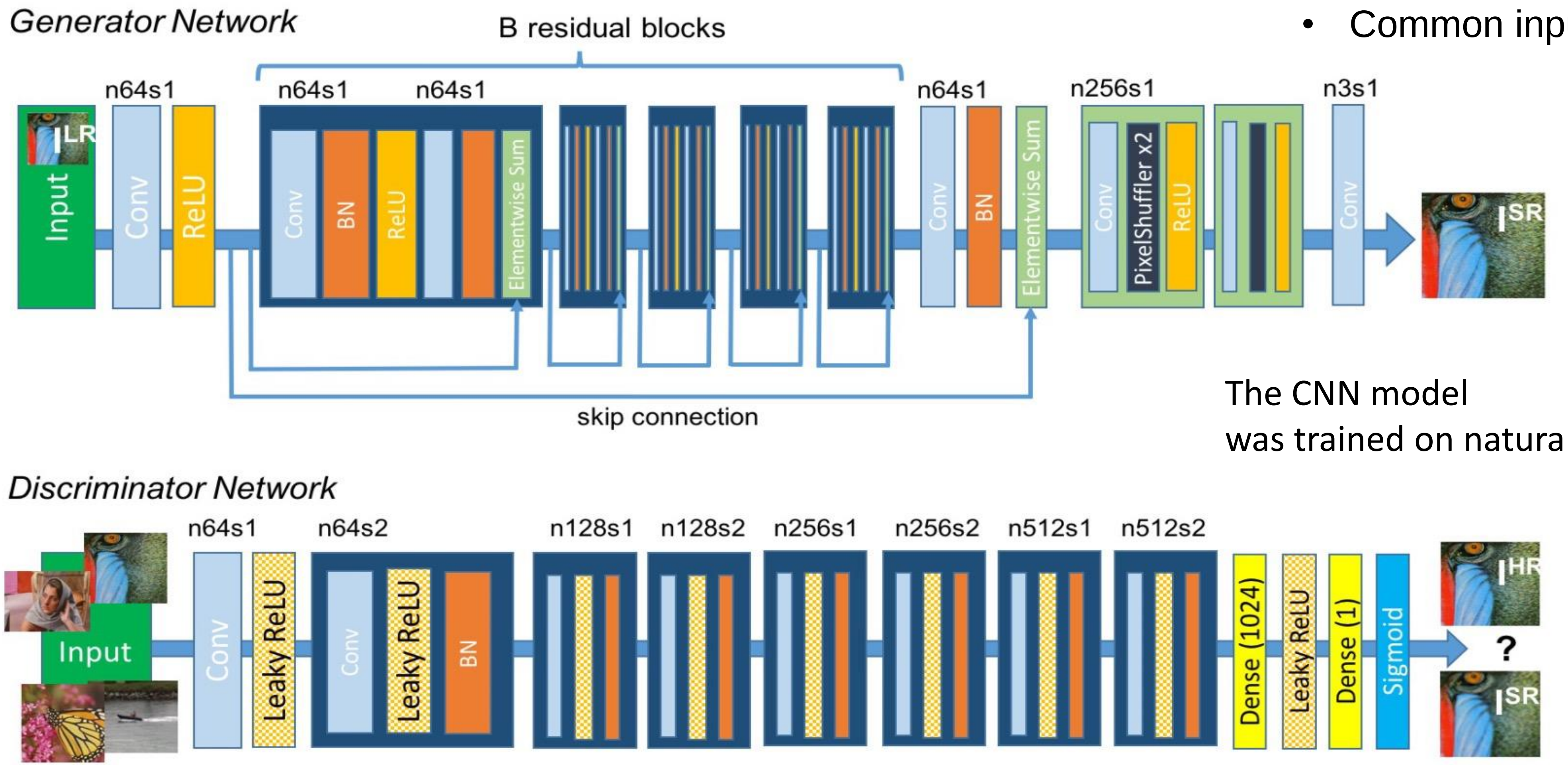

- SRGAN model → 1.55M parameters
- Common input shape → (512×512)

The CNN model
was trained on natural images (DIV2K dataset)

First Results

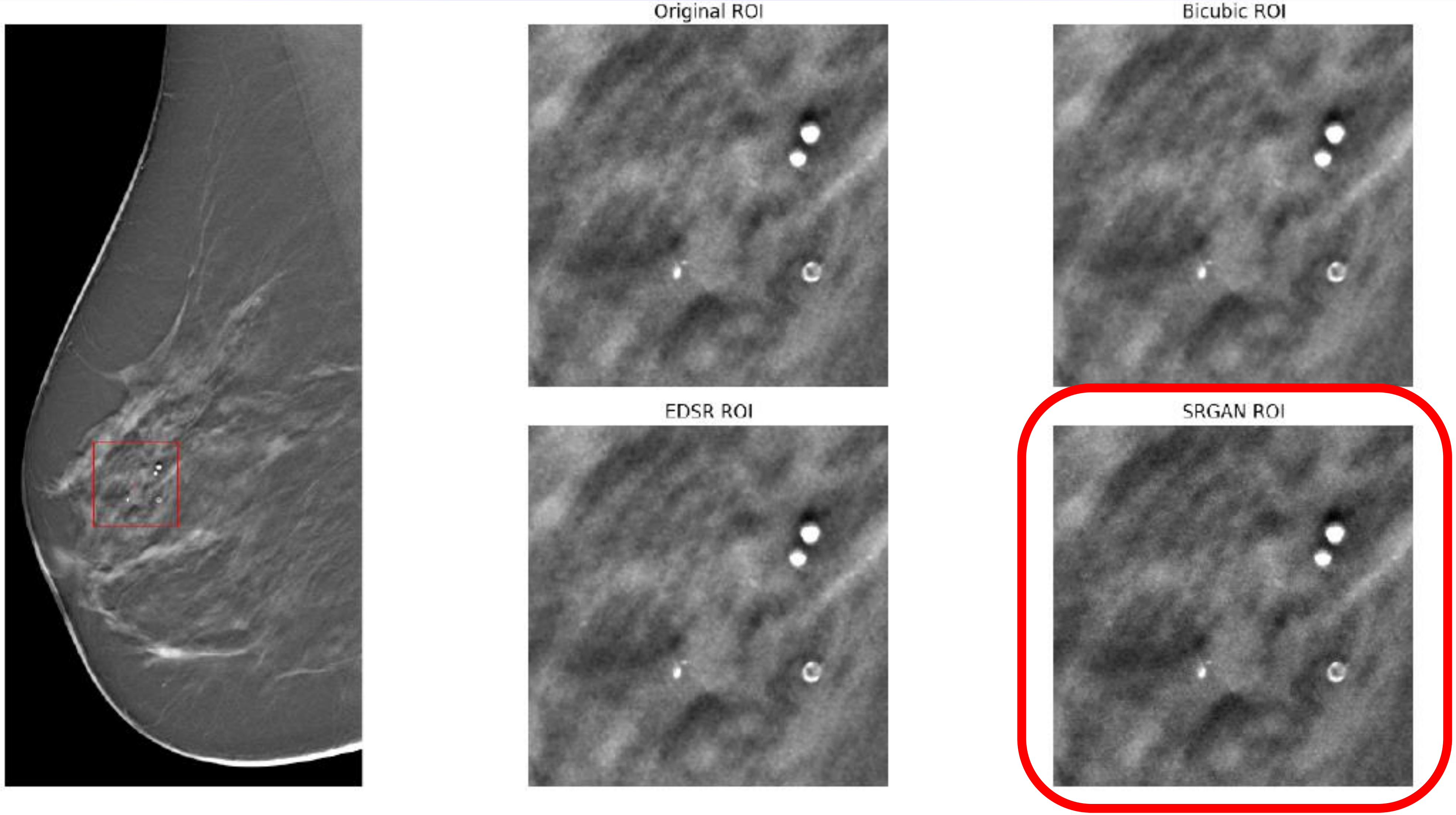

Super Resolution workflow

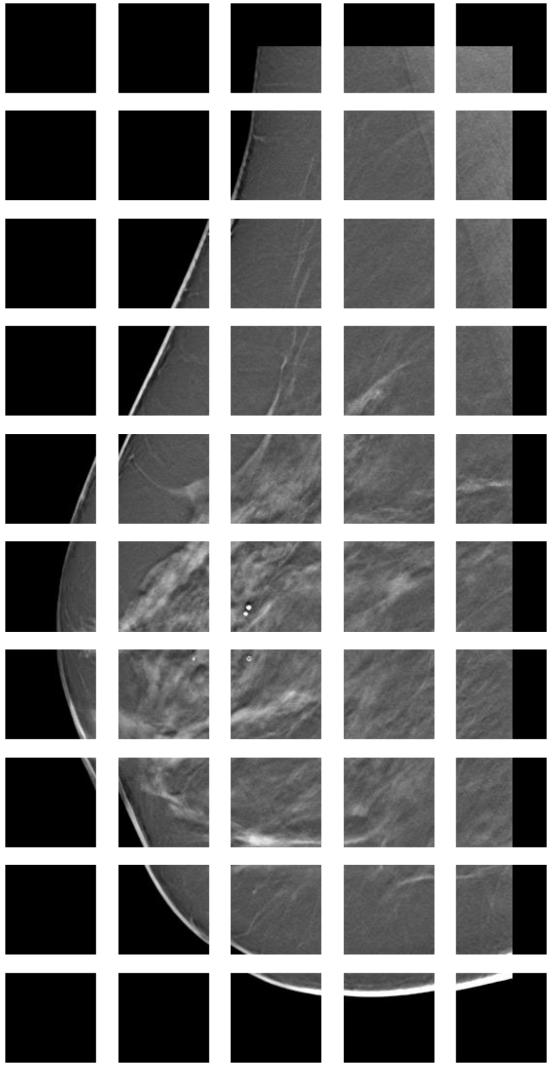

- Current input shape 2400×1100 ← **<u>unfeasible</u>**
- Split image into a series of disjointed patches (256×256)
- <u>Monitor the boundary effect related to image reconstruction</u>

Computational time requires for the SR of the entire image is around 7s

Examples

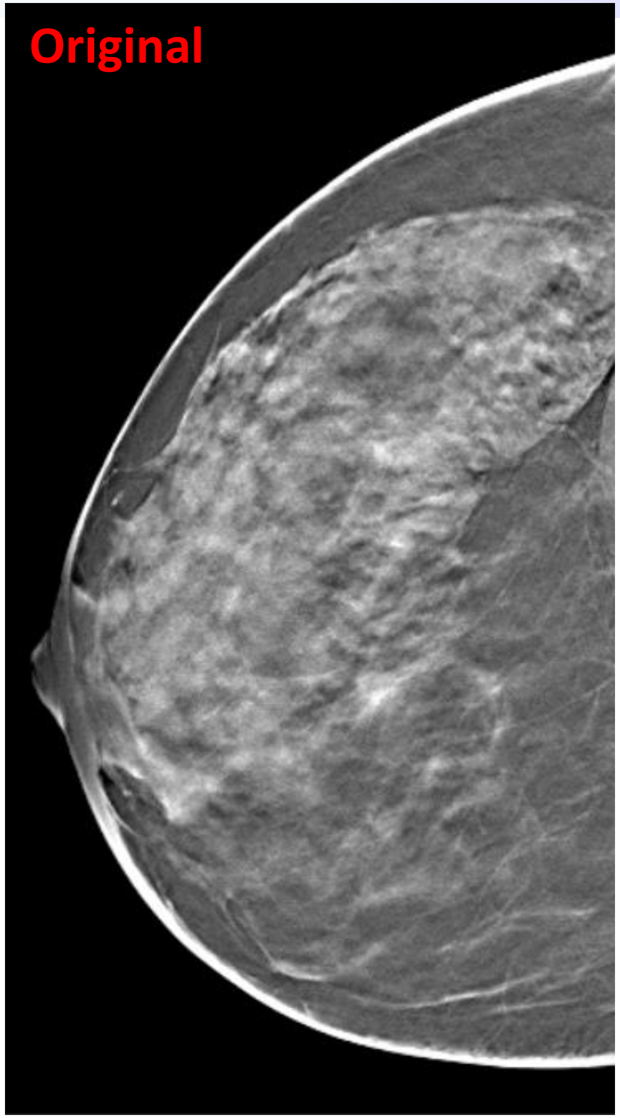

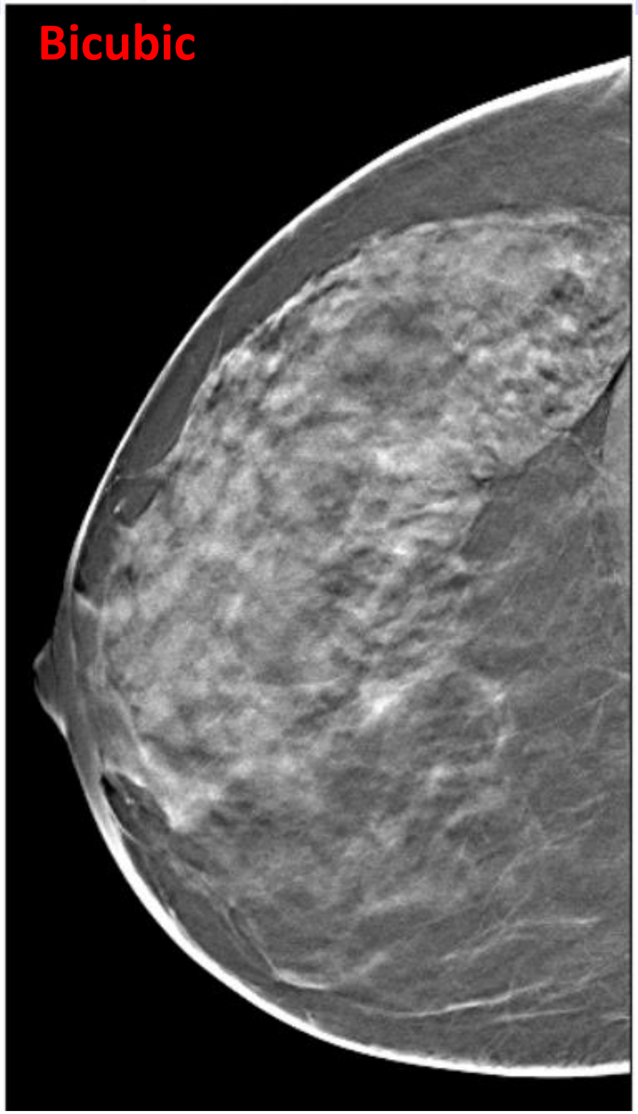

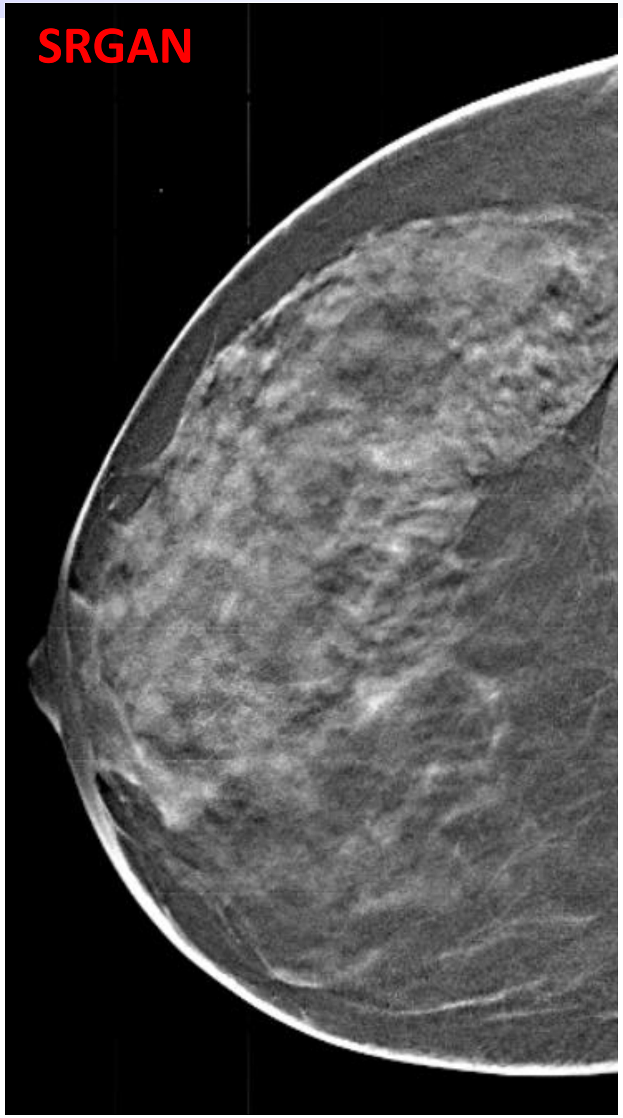

DeepLook

Pre-Processing	Slice Selection	Mass Localization	Flase Positive reduction	Super Resolution
Image enhancement	CC geometry	CC geometry	Radiomics	Transfer Learning test
	MLO geometry	MLO geometry		

Grazie per l’attenzione

Prof. Giovanni Mettivier
Associate Professor of Applied Physics
Medical Physics Specialist
Local Coordinator of INFN Technological Research